Arch Appl Mech (2013) 83:73–95
DOI 10.1007/s00419-012-0633-5

ORIGINAL

Yue-Ting Zhou · Kang Yong Lee

Frictional contact of anisotropic piezoelectric materials indented by flat and semi-parabolic stamps

Received: 18 October 2011 / Accepted: 3 April 2012 / Published online: 26 April 2012

Abstract An exact analysis of frictional contact of anisotropic piezoelectric materials indented by a rigid flat or semi-parabolic stamp is conducted. Fundamental solutions that can lead to the real values of physical quantities are detailed for each eigenvalue distribution. The complicated mixed boundary value problems are reduced into a singular integral equation of the second kind in terms of the unknown surface contact stress beneath the stamp. Employing excellent properties of Jacobi Polynomials, the exact solution of the reduced second kind singular integral equation can be obtained. Exact and explicit expressions of various surface stresses and electric displacement are given in terms of elementary functions. Relationships between the applied load and contact area are derived, and stress intensity factors at stamp edges are given. Numerical results are presented to show the effects of the friction coefficient on various surface stresses and electric displacement. The present investigation could provide a scientific basis for the theoretical and experimental test of contact behaviors of anisotropic piezoelectric materials.

Keywords Frictional contact · Anisotropic piezoelectric materials · Rigid stamp · Singular integral equation · Exact solutions

1 Introduction

Piezoelectric materials can deform when subjected to an electric field and, conversely, they generate electric charge when subjected to a mechanical loading (Sosa and Castro [19]). Due to their coupling electromechanical properties, piezoelectric materials are widely used in sensors and actuators in the field of smart materials and structures. A lot of theoretical studies on piezoelectric materials have been done, e.g. Ding et al. [3–5].

However, subjected to a highly localized loading exerted by a rigid body, piezoelectric materials could lose their serviceability. Thus, contact problems of piezoelectric materials have drawn much attention of researchers. Matysiak [15] investigated contact over a piezoelectro-elastic half-space indented by a rigid conducting stamp. Podilchuk and Tkachenko [16] obtained the explicit solution of the problem of a rigid stamp with a semi-parabolic cross-section and flat base pressed into an elastic piezoelectric ceramic half-space. Giannakopoulos and Suresh [8] presented a general theory for the axisymmetric indentation of piezoelectric solids within the contexts of conducting and insulting stamps. Chen [1] conducted a contact analysis for a three-dimensional transversely isotropic piezoelectric half-space. Ramirez and Heyliger [18] applied the local/global stiffness matrix framework to investigate the contact problem with piezoelectric materials exhibiting hexagonal symmetry, which generate only real eigenvalues. Later, Ramirez [17] used the same approach to investigate the

Y.-T. Zhou · K. Y. Lee (✉)
School of Mechanical Engineering, Yonsei University, Seoul 120-749, Republic of Korea
E-mail: KYL2813@yonsei.ac.kr; KYL2813@gmail.com

K. Y. Lee
Department of Engineering Mechanics, Dalian University of Technology, DaLian 116024, People's Republic of China

contact problem with piezoelectric materials, which can generate complex eigenvalues. Wang and Han [22] gave exact solutions of the axisymmetric contact problem of a piezoelectric layer with a circular indenter on its surface. Recently, Wang et al. [23] investigated the contact of a piezoelectric layer with a finite thickness indented by insulting or conducting stamps on its surface, in which thickness effect on contact behavior was addressed. All above-mentioned contact problems involving piezoelectric materials were smooth.

Frictional shear stress may arise inside the contact region between rigid stamp and piezoelectric materials. Thus, some researchers devoted to frictional contact problems of piezoelectric materials. For example, Karapetian et al. [12] conducted nanoelectromechanics analysis of frictional piezoelectric indentation. Makagon et al. [14] addressed the indentation and frictional sliding of spherical and conical stamps into piezoelectric half-space. Contact problems of inhomogeneous piezoelectric materials were also concerned. For example, Ke et al. [13] considered the frictional contact of the inhomogeneous piezoelectric layered half-plane.

All the contact problems mentioned above were about transversely isotropic piezoelectric materials. However, piezoelectric materials are naturally anisotropic. Therefore, the anisotropy of piezoelectric materials should be considered. Relatively few discussions have been devoted to contact problems of anisotropic piezoelectric materials. Employing Stroh's formalism, Chung and Ting [2] studied the problems of an angularly inhomogeneous anisotropic piezoelectric materials subjected to a line force, line charge, and line dislocation at the center of the material. Fan et al. [7] used a Stroh formalism approach to solve the two-dimensional contact problem of a piezoelectric half-plane and obtained solutions with loads acting on the boundary of an anisotropic piezoelectric half-plane. To the authors' knowledge, the exact solution of the frictional contact problem of anisotropic piezoelectric materials subjected to a rigid stamp has not been reported due to its complexity.

In the present paper, an exact analysis of frictional contact of anisotropic piezoelectric materials under a rigid stamp, which possesses a flat or semi-parabolic profile, is conducted. For the commercially available anisotropic piezoelectric materials, there are three cases of eigenvalue distribution. For each case, fundamental solutions that can lead to real values of physical quantities are derived. The titled problem is reduced into a second kind singular integral equation, which can be solved exactly by using excellent properties of Jacobi Polynomials. Explicit expressions of various surface stresses and electric displacement are given in elementary functions for either a flat stamp or a semi-parabolic stamp. Relationships between the applied mechanical loading and the contact area are presented, and stress intensity factors at stamp edges are defined. Figures are plotted to show the influences of the friction coefficient on various surface stresses and electric displacement. The present results could provide a theoretical basis for contact behaviors of anisotropic piezoelectric materials.

2 Basic equations

To illustrate the problem considered in this study, Fig. 1 shows the indentation problem of a semi-finite anisotropic piezoelectric material under a rigid stamp, which possesses a flat or semi-parabolic profile. The anisotropic piezoelectric materials, placed in rectangular coordinates, are poled along the positive z axis. It is modeled that the stamp and anisotropic piezoelectric materials are in relative motion, that is,

$$Q = \mu_f \cdot P$$

where μ_f is the coefficient of friction, which is a constant inside the contact area; P and Q are the resultant normal and tangential forces, respectively.

For anisotropic piezoelectric materials, the coupled constitutive equations are given as

$$\sigma_{ij} = C_{ijkl}\varepsilon_{kl} + e_{ijk}\phi_{,k} \tag{1}$$

$$D_i = e_{ikl}\varepsilon_{kl} - \in_{ik} \phi_{,k} \tag{2}$$

where σ_{ij} is stress component, D_i is electric displacement component, ϕ represents the electric potential, and C_{ijkl}, e_{ikl}, and $\in_{ik}$ stand for the elastic coefficients, piezoelectric coefficients, and dielectric coefficients, respectively. The subscript after a comma represents partial differentiation. The strain ε_{kl} is given by

$$\varepsilon_{kl} = \frac{1}{2}\left(u_{k,l} + u_{l,k}\right) \tag{3}$$

where u_i is displacement components.

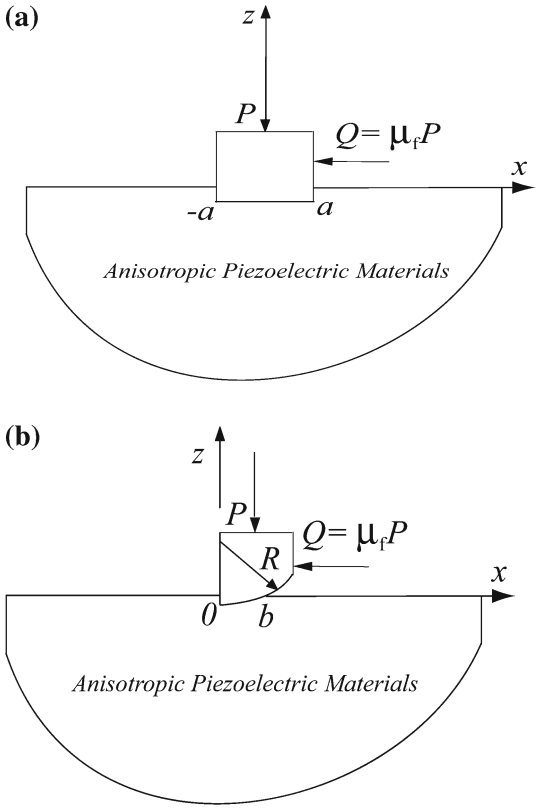

Fig. 1 Geometry of the frictional contact problem of anisotropic piezoelectric materials indented by: **a** a flat stamp, **b** a semi-parabolic stamp

The equations of equilibrium and Maxwell's equation without generalized body force are given as follows:

$$\sigma_{ij,j} = 0 \tag{4}$$

$$D_{i,i} = 0 \tag{5}$$

In the present study, since sliding contact model is assumed, Eq. (5) is of static state and relative velocity does not appear.

For a two-dimensional y-independent problem, a generalized deformation field is expressed as

$$u = u_1(x, z),\ v = u_2(x, z),\ w = u_3(x, z),\ \phi = \phi(x, z)$$

Inserting constitution Eqs. (1) and (2) into Eqs.(4) and (5) leads to the following governing equations for the anisotropic piezoelectric materials in terms of elastic displacements and electric potential (Tiersten [20], Ramirez and Heylinger [18], Ramirez [17]):

$$c_{11}\frac{\partial^2 u}{\partial x^2} + c_{55}\frac{\partial^2 u}{\partial z^2} + c_{16}\frac{\partial^2 v}{\partial x^2} + c_{45}\frac{\partial^2 v}{\partial z^2} + (c_{13} + c_{55})\frac{\partial^2 w}{\partial x \partial z} + (e_{31} + e_{15})\frac{\partial^2 \phi}{\partial x \partial z} = 0 \tag{6}$$

$$c_{16}\frac{\partial^2 u}{\partial x^2} + c_{45}\frac{\partial^2 u}{\partial z^2} + c_{66}\frac{\partial^2 v}{\partial x^2} + c_{44}\frac{\partial^2 v}{\partial z^2} + (c_{36} + c_{45})\frac{\partial^2 w}{\partial x \partial z} + (e_{36} + e_{14})\frac{\partial^2 \phi}{\partial x \partial z} = 0 \tag{7}$$

$$(c_{13} + c_{55})\frac{\partial^2 u}{\partial x \partial z} + (c_{36} + c_{45})\frac{\partial^2 v}{\partial x \partial z} + c_{55}\frac{\partial^2 w}{\partial x^2} + c_{33}\frac{\partial^2 w}{\partial z^2} + e_{15}\frac{\partial^2 \phi}{\partial x^2} + e_{33}\frac{\partial^2 \phi}{\partial z^2} = 0 \tag{8}$$

$$(e_{15} + e_{31})\frac{\partial^2 u}{\partial x \partial z} + (e_{14} + e_{36})\frac{\partial^2 v}{\partial x \partial z} + e_{15}\frac{\partial^2 w}{\partial x^2} + e_{33}\frac{\partial^2 w}{\partial z^2} - \epsilon_{11}\frac{\partial^2 \phi}{\partial x^2} - \epsilon_{33}\frac{\partial^2 \phi}{\partial z^2} = 0 \tag{9}$$

Note for convenience, C_{ijkl} and e_{ikl} in Eqs. (1) and (2) are replaced by c_{mn} and e_{mn} in Eqs. (6–9) and thereafter, respectively.

3 Fundamental solutions

3.1 Eigenvalue analysis

The solutions of Eqs. (7–9) may be written in the following forms:

$$u(x,z) = \int_{-\infty}^{\infty} U_{c\omega}(\omega,z)\, e^{-i\omega x}\mathrm{d}\omega, \qquad v(x,z) = \int_{-\infty}^{\infty} V_{c\omega}(\omega,z)\, e^{-i\omega x}\mathrm{d}\omega$$

$$w(x,z) = \int_{-\infty}^{\infty} W_{c\omega}(\omega,z)\, e^{-i\omega x}\mathrm{d}\omega \tag{10}$$

$$\phi(x,z) = \int_{-\infty}^{\infty} \Phi_{c\omega}(\omega,z)\, e^{-i\omega x}\mathrm{d}\omega \tag{11}$$

where $i^2 = -1$.

Substituting Eqs. (10) and (11) into the piezoelectric governing equations (6–9) yields the following equations:

$$-\omega^2 c_{11}U_{c\omega} + c_{55}\frac{\partial^2 U_{c\omega}}{\partial z^2} - \omega^2 c_{16}V_{c\omega} + c_{45}\frac{\partial^2 V_{c\omega}}{\partial z^2} - i\omega(c_{13}+c_{55})\frac{\partial W_{c\omega}}{\partial z}$$
$$-i\omega(e_{31}+e_{15})\frac{\partial \Phi_{c\omega}}{\partial z} = 0 \tag{12}$$

$$-\omega^2 c_{16}U_{c\omega} + c_{45}\frac{\partial^2 U_{c\omega}}{\partial z^2} - \omega^2 c_{66}V_{c\omega} + c_{44}\frac{\partial^2 V_{c\omega}}{\partial z^2} - i\omega(c_{36}+c_{45})\frac{\partial W_{c\omega}}{\partial z}$$
$$-i\omega(e_{36}+e_{14})\frac{\partial \Phi_{c\omega}}{\partial z} = 0 \tag{13}$$

$$-i\omega(c_{13}+c_{55})\frac{\partial U_{c\omega}}{\partial z} - i\omega(c_{36}+c_{45})\frac{\partial V_{c\omega}}{\partial z} - \omega^2 c_{55}W_{c\omega} + c_{33}\frac{\partial^2 W_{c\omega}}{\partial z^2}$$
$$-\omega^2 e_{15}\Phi_{c\omega} + e_{33}\frac{\partial^2 \Phi_{c\omega}}{\partial z^2} = 0 \tag{14}$$

$$-i\omega(e_{15}+e_{31})\frac{\partial U_{c\omega}}{\partial z} - i\omega(e_{14}+e_{36})\frac{\partial V_{c\omega}}{\partial z} - \omega^2 e_{15}W_{c\omega} + e_{33}\frac{\partial^2 W_{c\omega}}{\partial z^2} + \omega^2 \in_{11} \Phi_{c\omega}$$
$$- \in_{33} \frac{\partial^2 \Phi_{c\omega}}{\partial z^2} = 0 \tag{15}$$

The solutions of Eqs. (12–15) in the transformed domain are sought in the forms of

$$\left[\, U_{c\omega}(\omega,z)\ V_{c\omega}(\omega,z)\ W_{c\omega}(\omega,z)\ \Phi_{c\omega}(\omega,z) \,\right]^T = \left[\, U^0_{c\omega}\ V^0_{c\omega}\ W^0_{c\omega}\ \Phi^0_{c\omega} \,\right]^T e^{|\omega|\eta z}$$

where the superscript "T" stands for the transposition of a vector, and unknown Fourier coefficients $U^0_{c\omega}$, $V^0_{c\omega}$, $W^0_{c\omega}$, and $\Phi^0_{c\omega}$ are related to the following equation:

$$G \times \left[\, U^0_{c\omega}\ V^0_{c\omega}\ W^0_{c\omega}\ \Phi^0_{c\omega} \,\right]^T = 0 \tag{16}$$

with the matrix $G = (g_{mn})\,(m,n = 1,2,3,4)$ given in Appendix, and the eigenvalue η is the root of the following characteristic equation:

$$\det[G] = 0 \tag{17}$$

For a semi-infinite piezoelectric material, the following conditions at infinity should be fulfilled:

$$u(x,z), v(x,z), w(x,z), \phi(x,z) \to 0, \qquad \sqrt{x^2+z^2} \to \infty$$

It deserves emphasizing that the solution is three-dimensional in the sense that the displacement component $v(x, z)$ along y axis is nonzero because of the anisotropy of the material. Thus, the characteristic equation Eq. (17) is of eight-degree, and there are three cases of eigenvalue distribution available for semi-infinite anisotropic piezoelectric materials. While for isotropic piezoelectric materials, the corresponding characteristic equation is of six-degree and there are only two cases (Zhou and Lee [24]) of eigenvalue distribution available.

For the commercially available piezoelectric materials, the eigenvalues, which are usually distinctive, are of the following forms:

– **Case A**: four pairs of opposite real roots

$$\eta_1 = -\eta_5 = o_1, \eta_2 = -\eta_6 = o_2, \eta_3 = -\eta_7 = o_3, \eta_4 = -\eta_8 = o_4 \tag{18}$$

– **Case B**: two pairs of opposite real roots and two pairs of complex conjugate roots (no purely imaginary roots)

$$\eta_1 = -\eta_5 = o_1, \eta_2 = -\eta_6 = o_2, \eta_3 = -\eta_7 = o_3 + i\sigma_3, \eta_4 = -\eta_8 = o_3 - i\sigma_3 \tag{19}$$

– **Case C**: four pairs of complex conjugate roots (no purely imaginary roots)

$$\eta_1 = -\eta_5 = o_1 + i\sigma_1, \eta_2 = -\eta_6 = o_1 - i\sigma_1, \eta_3 = -\eta_7 = o_3 + i\sigma_3 \quad \eta_4 = -\eta_8 = o_3 - i\sigma_3 \tag{20}$$

In Eqs. (18–20) $o_n > 0$ and $\sigma_n > 0 (n = 1, 2, 3, 4)$ are real numbers.

3.2 Fundamental solutions

For each case of the eigenvalue distribution, the fundamental solutions $[U_{c\omega}(\omega, z) V_{c\omega}(\omega, z) W_{c\omega}(\omega, z) \Phi_{c\omega}(\omega, z)]^T$ can be given.

– **Case A**: four pairs of opposite real roots

$$U_{c\omega}(\omega, z) = \sum_{j=1}^{4} M_j e^{|\omega| o_j z}, \; V_{c\omega}(\omega, z) = \sum_{j=1}^{4} f(o_j) M_j e^{|\omega| o_j z}$$

$$W_{c\omega}(\omega, z) = \sum_{j=1}^{4} -i\,\mathrm{sgn}(\omega) g(o_j) M_j e^{|\omega| o_j z} \tag{21}$$

$$\Phi_{c\omega}(\omega, z) = \sum_{j=1}^{4} -i\,\mathrm{sgn}(\omega) h(o_j) M_j e^{|\omega| o_j z} \tag{22}$$

where known functions $f(\eta)$, $g(\eta)$ and $h(\eta)$ are given as

$$f(\eta) = f_0(\eta)/f_D(\eta), g(\eta) = g_0(\eta)/f_D(\eta), h(\eta) = h_0(\eta)/f_D(\eta) \tag{23}$$

Here $f_0(\eta)$, $f_D(\eta)$, $g_0(\eta)$ and $h_0(\eta)$ are given in Appendix.

– **Case B**: two pairs of opposite real roots and two pairs of complex conjugate roots (no purely imaginary roots)

$$
\begin{aligned}
U_{c\omega}(\omega,z) &= \sum_{j=1}^{2} M_j e^{|\omega| o_j z} + \left[\cos(|\omega|\,\sigma_3 z) M_3 + \sin(|\omega|\,\sigma_3 z) M_4\right] e^{|\omega| o_3 z} \\
V_{c\omega}(\omega,z) &= \sum_{j=1}^{2} f(o_j) M_j e^{|\omega| o_j z} + \{[\Gamma_V \cos(|\omega|\,\sigma_3 z) - \Delta_V \sin(|\omega|\,\sigma_3 z)] \\
&\quad M_3 + [\Delta_V \cos(|\omega|\,\sigma_3 z) + \Gamma_V \sin(|\omega|\,\sigma_3 z)]\, M_4\}\, e^{|\omega| o_3 z} \qquad (24) \\
W_{c\omega}(\omega,z) &= \sum_{j=1}^{2} \left[-i \cdot \mathrm{sgn}(\omega) g(o_j) M_j e^{|\omega| o_j z}\right] - i \cdot \mathrm{sgn}(\omega) \\
&\quad \{[\Gamma_W \cos(|\omega|\,\sigma_3 z) - \Delta_W \sin(|\omega|\,\sigma_3 z)]\, M_3 + [\Delta_W \cos(|\omega|\,\sigma_3 z) \\
&\quad + \Gamma_W \sin(|\omega|\,\sigma_3 z)]\, M_4\}\, e^{|\omega| o_3 z} \\
\Phi_{c\omega}(\omega,z) &= \sum_{j=1}^{2} \left[-i \cdot \mathrm{sgn}(\omega) h(o_j) M_j e^{|\omega| o_j z}\right] \\
&\quad - i \cdot \mathrm{sgn}(\omega)\, \{[\Gamma_\Phi \cos(|\omega|\,\sigma_3 z) - \Delta_\Phi \sin(|\omega|\,\sigma_3 z)]\, M_3 \\
&\quad + [\Delta_\Phi \cos(|\omega|\,\sigma_3 z) + \Gamma_\Phi \sin(|\omega|\,\sigma_3 z)]\, M_4\}\, e^{|\omega| o_3 z} \qquad (25)
\end{aligned}
$$

where

$$
\begin{aligned}
&\Gamma_V = \mathrm{Re}\left[f(\eta_3)\right], \Delta_V = \mathrm{Im}\left[f(\eta_3)\right], \Gamma_W = \mathrm{Re}\left[g(\eta_3)\right], \Delta_W = \mathrm{Im}\left[g(\eta_3)\right] \\
&\Gamma_\Phi = \mathrm{Re}\left[h(\eta_3)\right], \Delta_\Phi = \mathrm{Im}\left[h(\eta_3)\right], \eta_3 = o_3 + i\sigma_3
\end{aligned}
$$

Here, Re[] and Im[] stand for real part and imaginary part, respectively.

– **Case C**: four pairs of complex conjugate roots (no purely imaginary roots)

$$
\begin{aligned}
U_{c\omega}(\omega,z) &= \sum_{j=1}^{2} \left[\cos(|\omega|\,\sigma_{2j-1} z) M_{2j-1} + \sin(|\omega|\,\sigma_{2j-1} z) M_{2j}\right] e^{|\omega| o_{2j-1} z} \\
V_{c\omega}(\omega,z) &= \sum_{j=1}^{2} \left\{\left[\Gamma_V^{(j)} \cos(|\omega|\,\sigma_{2j-1} z) - \Delta_V^{(j)} \sin(|\omega|\,\sigma_{2j-1} z)\right] M_{2j-1}\right. \\
&\quad \left. + \left[\Delta_V^{(j)} \cos(|\omega|\,\sigma_{2j-1} z) + \Gamma_V^{(j)} \sin(|\omega|\,\sigma_{2j-1} z)\right] M_{2j}\right\} e^{|\omega| o_{2j-1} z} \qquad (26) \\
W_{c\omega}(\omega,z) &= \sum_{j=1}^{2} -i \cdot \mathrm{sgn}(\omega) \left\{\left[\Gamma_W^{(j)} \cos(|\omega|\,\sigma_{2j-1} z) - \Delta_W^{(j)} \sin(|\omega|\,\sigma_{2j-1} z)\right] M_{2j-1}\right. \\
&\quad \left. + \left[\Delta_W^{(j)} \cos(|\omega|\,\sigma_{2j-1} z) + \Gamma_W^{(j)} \sin(|\omega|\,\sigma_{2j-1} z)\right] M_{2j}\right\} e^{|\omega| o_{2j-1} z} \\
\Phi_{c\omega}(\omega,z) &= \sum_{j=1}^{2} -i \cdot \mathrm{sgn}(\omega) \left\{\left[\Gamma_\Phi^{(j)} \cos(|\omega|\,\sigma_{2j-1} z) - \Delta_\Phi^{(j)} \sin(|\omega|\,\sigma_{2j-1} z)\right] M_{2j-1}\right. \\
&\quad \left. + \left[\Delta_\Phi^{(j)} \cos(|\omega|\,\sigma_{2j-1} z) + \Gamma_\Phi^{(j)} \sin(|\omega|\,\sigma_{2j-1} z)\right] M_{2j}\right\} e^{|\omega| o_{2j-1} z} \qquad (27)
\end{aligned}
$$

where

$$
\begin{aligned}
&\Gamma_V^{(j)} = \mathrm{Re}\left[f\left(\eta_{2j-1}\right)\right], \Delta_V^{(j)} = \mathrm{Im}\left[f\left(\eta_{2j-1}\right)\right], \Gamma_W^{(j)} = \mathrm{Re}\left[g\left(\eta_{2j-1}\right)\right] \\
&\Delta_W^{(j)} = \mathrm{Im}\left[g\left(\eta_{2j-1}\right)\right], \Gamma_\Phi^{(j)} = \mathrm{Re}\left[h\left(\eta_{2j-1}\right)\right], \Delta_\Phi^{(j)} = \mathrm{Im}\left[h\left(\eta_{2j-1}\right)\right], j = 1, 2
\end{aligned}
$$

In Eqs. (21), (22) and (24–27), $M_j (j = 1, 2, 3, 4)$ are unknown functions to be determined from boundary conditions.

3.3 Expressions of physical quantities

Considering Eqs. (21), (22), (24–27), and substituting Eqs. (10) and (11) into Eqs. (1) and (2) yield the following expressions of stresses and electric displacement:

$$\sigma_{xx} = \int_{-\infty}^{\infty} \sum_{j=1}^{4} |\omega| \, \Omega_{0j}^{(s)}(\omega, z) M_j(\omega) e^{-i\omega x} \mathrm{d}\omega$$

$$\sigma_{zz} = \int_{-\infty}^{\infty} \sum_{j=1}^{4} |\omega| \, \Omega_{1j}^{(s)}(\omega, z) M_j(\omega) e^{-i\omega x} \mathrm{d}\omega$$

$$\sigma_{xz} = \int_{-\infty}^{\infty} \sum_{j=1}^{4} |\omega| \, \Omega_{2j}^{(s)}(\omega, z) M_j(\omega) e^{-i\omega x} \mathrm{d}\omega$$

$$\sigma_{yz} = \int_{-\infty}^{\infty} \sum_{j=1}^{4} |\omega| \, \Omega_{3j}^{(s)}(\omega, z) M_j(\omega) e^{-i\omega x} \mathrm{d}\omega \tag{28}$$

$$D_x = \int_{-\infty}^{\infty} \sum_{j=1}^{4} |\omega| \, \Omega_{0j}^{(e)}(\omega, z) M_j(\omega) e^{-i\omega x} \mathrm{d}\omega$$

$$D_z = \int_{-\infty}^{\infty} \sum_{j=1}^{4} |\omega| \, \Omega_{1j}^{(e)}(\omega, z) M_j(\omega) e^{-i\omega x} \mathrm{d}\omega \tag{29}$$

where known functions $\Omega_{mj}^{(s)}(\omega, z)(m = 0, 1, 2, 3, j = 1, 2, 3, 4)$ and $\Omega_{nj}^{(e)}(\omega, z)(n = 0, 1, j = 1, 2, 3, 4)$ are given in Appendix.

3.4 Boundary conditions

The vertical displacement inside the contact area is denoted as $w_0(x)$, which is known a priori. The surface contact stress $p(x)$ and surface shear stress $q(x)$ are unknown inside the contact area. Outside the contact area, the stress is free. The total force along the z axis in the contact area is equal to the indentation force P.

$$w(x, 0) = w_0(x), \ -a < x < b \tag{30}$$

$$\sigma_{zz}(x, 0) = -p(x), \ -a < x < b \tag{31}$$

$$\sigma_{zz}(x, 0) = 0, \ x < -a \ or \ x > b \tag{32}$$

$$\sigma_{xz}(x, 0) = -q(x), \ -a < x < b \tag{33}$$

$$\sigma_{xz}(x, 0) = 0, \ x < -a \ or \ x > b \tag{34}$$

$$\sigma_{yz}(x, 0) = 0, \ |x| < +\infty \tag{35}$$

$$\int_{-a}^{b} p(x) \mathrm{d}x = P \tag{36}$$

Coulomb friction condition is modeled inside the contact area, and then the following condition should be satisfied

$$\sigma_{xz}(x, 0) = \mu_f \sigma_{zz}(x, 0), \ -a < x < b \tag{37}$$

For a perfectly insulating stamp, the electric boundary condition is given as follows:

$$D_z(x,0)=0,\ |x|<\infty \tag{38}$$

Considering the boundary conditions (31–35), (37), and (38) yields the following expressions for unknown functions M_j $(j=1,2,3,4)$:

$$M_j=\frac{(-1)^j}{|\omega|H}\left[F_f(\omega)H_{1j}-G_f(\omega)H_{2j}\right],\ j=1,2,3,4 \tag{39}$$

where H is the determinant and $H_{ij}(i,j=1,2,3,4)$ are the cofactors of the following matrix:

$$M_H=\begin{bmatrix}\Omega_{11}^{(s)}(\omega,0)&\Omega_{12}^{(s)}(\omega,0)&\Omega_{13}^{(s)}(\omega,0)&\Omega_{14}^{(s)}(\omega,0)\\ \Omega_{21}^{(s)}(\omega,0)&\Omega_{22}^{(s)}(\omega,0)&\Omega_{23}^{(s)}(\omega,0)&\Omega_{24}^{(s)}(\omega,0)\\ \Omega_{31}^{(s)}(\omega,0)&\Omega_{32}^{(s)}(\omega,0)&\Omega_{33}^{(s)}(\omega,0)&\Omega_{34}^{(s)}(\omega,0)\\ \Omega_{11}^{(e)}(\omega,0)&\Omega_{12}^{(e)}(\omega,0)&\Omega_{13}^{(e)}(\omega,0)&\Omega_{14}^{(e)}(\omega,0)\end{bmatrix}$$

and functions F_f and G_f are given as follows:

$$F_f(\omega)=\frac{1}{2\pi}\int_{-a}^{b}p(\xi)e^{i\omega\xi}\mathrm{d}\xi,\ G_f(\omega)=\frac{1}{2\pi}\int_{-a}^{b}q(\xi)e^{i\omega\xi}\mathrm{d}\xi$$

4 Integral equations

Inspecting the third equation of Eqs. (21), (24), (26), and (39), and differentiating the third equation of Eq. (10) lead to the following equation:

$$\frac{\partial w(x,0)}{\partial x}=\frac{1}{\pi}\int_{-a}^{b}\int_{0}^{\infty}\left\{L_{11}\sin\left[\omega(\xi-x)\right]p(\xi)+L_{12}\cos\left[\omega(\xi-x)\right]q(\xi)\right\}\mathrm{d}\omega\mathrm{d}\xi\qquad|x|<\infty$$

Due to their physical interest, the in-plane stress on the surface and in-plane electric displacement can also be obtained as

$$\sigma_{xx}(x,0)=\frac{1}{\pi}\int_{-a}^{b}\int_{0}^{\infty}\left\{L_{21}\cos\left[\omega(\xi-x)\right]p(\xi)+L_{22}\sin\left[\omega(\xi-x)\right]q(\xi)\right\}\mathrm{d}\omega\mathrm{d}\xi\qquad|x|<\infty$$

$$D_x(x,0)=\frac{1}{\pi}\int_{-a}^{b}\int_{0}^{\infty}\left\{L_{31}\sin\left[\omega(\xi-x)\right]p(\xi)+L_{32}\cos\left[\omega(\xi-x)\right]q(\xi)\right\}\mathrm{d}\omega\mathrm{d}\xi\qquad|x|<\infty$$

where

$$\begin{aligned}L_{11}&=\sum_{j=1}^{4}(-1)^j\Theta_j(\omega,0)\frac{H_{1j}}{H},\ L_{12}=i\sum_{j=1}^{4}(-1)^j\Theta_j(\omega,0)\frac{H_{2j}}{H}\\ L_{21}&=\sum_{j=1}^{4}(-1)^j\Omega_{0j}^{(s)}(\omega,0)\frac{H_{1j}}{H},\ L_{22}=i\sum_{j=1}^{4}(-1)^{j+1}\Omega_{0j}^{(s)}(\omega,0)\frac{H_{2j}}{H}\\ L_{31}&=i\sum_{j=1}^{4}(-1)^j\Omega_{0j}^{(e)}(\omega,0)\frac{H_{1j}}{H},\ L_{32}=\sum_{j=1}^{4}(-1)^{j+1}\Omega_{0j}^{(e)}(\omega,0)\frac{H_{2j}}{H}\end{aligned} \tag{40}$$

where $\Theta_j(\omega,0)(j=1,2,3,4)$ are the values of $\Theta_j(\omega,z)$ $(j=1,2,3,4)$ at $z=0$ and $\Theta_j(\omega,z)(j=1,2,3,4)$ are given in Appendix.

Considering the following relations:

$$\int_0^\infty \sin\left[\omega\left(\xi-x\right)\right]\mathrm{d}\omega=\frac{1}{\xi-x},\qquad \int_0^\infty \cos\left[\omega\left(\xi-x\right)\right]\mathrm{d}\omega=\pi\delta\left(\xi-x\right)$$

where $\delta(\cdot)$ is the Dirac delta function, and taking into account Eq. (37) produce the following second type singular integral equation:

$$\frac{\partial w\left(x,0\right)}{\partial x}=L_{12}\mu_f p(x)+\frac{1}{\pi}\int_{-a}^{b}\frac{L_{11}}{\xi-x}p(\xi)\mathrm{d}\xi,\qquad |x|<\infty \tag{41}$$

To complete the stated problem, the equilibrium condition (36) should be fulfilled. Based on the solution of Eqs. (41) and (36), the in-plane stress and in-plane electric displacement on the surface can be determined as

$$\sigma_{xx}\left(x,0\right)=L_{21}p(x)+\frac{1}{\pi}\int_{-a}^{b}\frac{L_{22}}{\xi-x}\mu_f p(\xi)\mathrm{d}\xi,\qquad |x|<\infty \tag{42}$$

$$D_x\left(x,0\right)=L_{32}\mu_f p(x)+\frac{1}{\pi}\int_{-a}^{b}\frac{L_{31}}{\xi-x}p(\xi)\mathrm{d}\xi,\qquad |x|<\infty \tag{43}$$

Note that in Eqs. (41–43) $p(x)=q(x)=0$ for $x\notin[-a,b]$, and they are the extensions of Galin's equations [11] for classical elasticity to piezoelectric media.

5 Exact solutions for a frictional flat stamp

The indentation depth appearing in Eq. (30) is of a constant value inside the contact region for a flat stamp, then

$$w_0\left(x\right)=\text{constant},\qquad \frac{\partial w_0\left(x\right)}{\partial x}=0$$

Noting $b=a$ and introducing the following normalized quantities:

$$x=as,\xi=a\zeta,\qquad -a<(x,\xi)<a,-1<(s,\zeta)<1\qquad p(x)=\varphi(s) \tag{44}$$

then Eqs. (41) and (36) can be written as

$$L_{12}\cdot\mu_f\cdot\varphi(s)+\frac{1}{\pi}\int_{-1}^{1}\frac{L_{11}}{\zeta-s}\varphi(\zeta)\mathrm{d}\zeta=0,\qquad |s|<1 \tag{45}$$

$$\int_{-1}^{1}\varphi(\zeta)\mathrm{d}\zeta=\frac{P}{a} \tag{46}$$

The solution to Eqs. (45) and (46) may be expressed as the following form in terms of Jacobi Polynomials (Erdogan [6]):

$$\varphi(\zeta)=\varpi(\zeta)\sum_{j=0}^{\infty}c_j P_j^{(\tau,\vartheta)}(\zeta),\qquad |\zeta|<1 \tag{47}$$

where $c_j (j \geq 0)$ is unknown coefficient to be determined, and $\varpi(\zeta)$ is the weight function and is given as

$$\varpi(\zeta) = (1-\zeta)^{\tau}(1+\zeta)^{\vartheta}, \qquad |\zeta| < 1 \tag{48}$$

where $P_j^{(\tau,\vartheta)}(\cdot)$ are Jacobi Polynomials related to the weight function $\varpi(\cdot)$.

The index of the integral equation is defined by

$$\kappa_0 = -(\tau + \vartheta) = 1$$

Due to the physics of the problem for the flat stamp, τ and ϑ are given as

$$\begin{aligned} &\varsigma > 0 : \tau = -\tfrac{\varepsilon}{\pi},\ \vartheta = \tfrac{\varepsilon}{\pi} - 1 \\ &\varsigma = 0 : \tau = -\tfrac{1}{2},\ \vartheta = -\tfrac{1}{2} \\ &\varsigma < 0 : \tau = \tfrac{\varepsilon}{\pi} - 1,\ \vartheta = -\tfrac{\varepsilon}{\pi} \end{aligned}$$

where

$$\varsigma = \tfrac{\mu_f L_{12}}{L_{11}},\ \tan\varepsilon = \left|\tfrac{1}{\varsigma}\right| \tag{49}$$

Considering the following property of Jacobi Polynomials:

$$\mu_f L_{12}\varpi(s)P_j^{(\tau,\vartheta)}(s) + \frac{L_{11}}{\pi}\int_{-1}^{1}\frac{\varpi(\zeta)P_j^{(\tau,\vartheta)}(\zeta)}{\zeta - s}\varphi(\zeta)\mathrm{d}\zeta = -\frac{L_{11}}{2^{\kappa_0}\sin(\pi\tau)}P_{j-1}^{(-\tau,-\vartheta)}(s),\ |s| < 1 \tag{50}$$

and inserting Eq. (47) into Eq. (45) lead to the following expression:

$$\sum_{j=1}^{\infty}\tfrac{-L_{11}}{2\sin(\pi\tau)}P_{j-1}^{(-\tau,-\vartheta)}(s)c_j = 0,\ |s| < 1$$

From the linear independence of the Jacobi Polynomials $P_j^{(\tau,\vartheta)}(\cdot)$, one may see Eq. (47) has only one nonzero coefficient c_0. Then, Eq. (47) becomes

$$\varphi(\zeta) = c_0(1-\zeta)^{\tau}(1+\zeta)^{\vartheta},\ |\zeta| < 1 \tag{51}$$

Substituting Eq. (51) into Eq. (46) and using the relation (here $\tau + \vartheta = -1$)

$$\int_{-1}^{1}\varpi(\zeta)\mathrm{d}\zeta = \frac{2^{\tau+\vartheta+1}\Gamma(\tau+1)\Gamma(\vartheta+1)}{\Gamma(\tau+\vartheta+2)} \tag{52}$$

one can determine the coefficient c_0 as follows:

$$c_0 = -\frac{2\sigma_0\sin(\pi\tau)}{\pi} \tag{53}$$

where

$$\sigma_0 = \frac{P}{2a}$$

Considering Eqs. (31), (44), (51), and (53), one can obtain the contact stress distribution

$$\sigma_{zz}(x,0) = \tfrac{2\sigma_0\sin(\pi\tau)}{\pi}(1-\tfrac{x}{a})^{\tau}(1+\tfrac{x}{a})^{\vartheta},\ |x| < a \tag{54}$$

With the consideration of Eq. (32), Eqs. (54) and (55) can be rewritten as

$$\sigma_{xx}(x,0)=\begin{cases} L_{21}p(x)+\frac{\mu_f}{\pi}\int\limits_0^a \frac{L_{22}}{\xi-x}p(\xi)\mathrm{d}\xi, & |x|>a \\ \frac{\mu_f}{\pi}\int\limits_0^a \frac{L_{22}}{\xi-x}p(\xi)\mathrm{d}\xi, & |x|<a \end{cases} \tag{55}$$

$$D_x(x,0)=\begin{cases} L_{32}\mu_f p(x)+\frac{1}{\pi}\int\limits_0^a \frac{L_{31}}{\xi-x}p(\xi)\mathrm{d}\xi, & |x|>a \\ \frac{1}{\pi}\int\limits_0^a \frac{L_{31}}{\xi-x}p(\xi)\mathrm{d}\xi, & |x|<a \end{cases} \tag{56}$$

Considering Eqs. (32), (42), and (43), one can rewrite Eqs. (55) and (56) in the following closed-form (Guler and Erdogan [9]):

$$\sigma_{xx}(x,0)=-\frac{2\sigma_0\sin(\pi\tau)}{\pi}\begin{cases} L_{21}(1-\frac{x}{a})^{\tau}(1+\frac{x}{a})^{\vartheta}+\frac{L_{22}\cdot\mu_f}{\pi}\mathrm{H}_L(x), & |x|<a \\ \frac{L_{22}\cdot\mu_f}{\pi}\mathrm{H}_L(x), & |x|>a \end{cases} \tag{57}$$

$$D_x(x,0)=-\frac{2\sigma_0\sin(\pi\tau)}{\pi}\begin{cases} L_{32}\mu_f(1-\frac{x}{a})^{\tau}(1+\frac{x}{a})^{\vartheta}+\frac{L_{31}}{\pi}\mathrm{H}_L(x), & |x|<a \\ \frac{L_{31}}{\pi}\mathrm{H}_L(x), & |x|>a \end{cases} \tag{58}$$

In Eqs. (57) and (58), $\mathrm{H}_L(x)$ is given as

$$\mathrm{H}_L(x)=\frac{\pi}{\sin(\pi\tau)}\begin{cases} -(1-\frac{x}{a})^{\tau}(-\frac{x}{a}-1)^{\vartheta}, & x<-a \\ (1-\frac{x}{a})^{\tau}(1+\frac{x}{a})^{\vartheta}\cos(\pi\tau), & -a<x<a \\ (\frac{x}{a}-1)^{\tau}(1+\frac{x}{a})^{\vartheta}, & x>a \end{cases}$$

The mode I stress intensity factor at the edges of the flat stamp can be defined as

$$F_I(a)=\lim_{x\to a}\frac{p(x)}{2^{\vartheta}}(a-x)^{-\tau}=\frac{c_0}{a^{\tau}} \tag{59}$$

$$F_I(-a)=\lim_{x\to -a}\frac{p(x)}{2^{\tau}}(a+x)^{-\vartheta}=\frac{c_0}{a^{\vartheta}} \tag{60}$$

The friction coefficient $\mu_f=0$ leads to $\tau=\vartheta=-1/2$, then Eqs. (59) and (60) become

$$F_I(a)=F_I(-a)=c_0\sqrt{a}=\frac{P}{\pi\sqrt{a}} \tag{61}$$

Especially, when friction coefficient $\mu_f=0$,, the surface contact stress (54) becomes

$$\sigma_{zz}(x,0)=-\frac{P}{\pi}\sqrt{a^2-x^2},\ |x|<a$$

This formula, dependent on applied load P, is just the same as the result for isotropic piezoelectric materials given by Wang et al. [23] (note in [23] $P_0=P/2$), which justifies our derivation.

6 Exact solutions for a frictional semi-parabolic stamp

The profile for a semi-parabolic stamp is given by

$$w_0(x)=-C_0+\frac{x^2}{2R},\ \frac{\partial w_0(x)}{\partial x}=\frac{x}{R},\qquad 0<x<b$$

Noting $a=0$ and defining

$$x=\frac{b}{2}(s+1),\ \xi=\frac{b}{2}(\zeta+1),\ p(x)=\varphi(s) \tag{62}$$

then Eqs. (41) and (36) can be written as

$$L_{12} \cdot \mu_f \cdot \varphi(s) + \frac{1}{\pi} \int_{-1}^{1} \frac{L_{11}}{\zeta - s} \varphi(\zeta) \mathrm{d}\zeta = \frac{b}{2R} g(s), \ |s| < 1 \tag{63}$$

$$\int_{-1}^{1} \varphi(\zeta) \mathrm{d}\zeta = \frac{2P}{b} \tag{64}$$

where

$$g(s) = s + 1$$

The solution of Eqs. (63) and (64) may be assumed as the same form given in Eq. (47) with eight function $\varpi(\cdot)$ given in Eq. (48).

The index of the semi-parabolic stamp is defined as

$$\kappa_0 = -(\tau + \vartheta) = 0$$

where τ and ϑ are given as follows:

$$\begin{aligned} &\varsigma > 0 : \tau = 1 - \tfrac{\varepsilon}{\pi}, \ \vartheta = -1 + \tfrac{\varepsilon}{\pi}, \\ &\varsigma = 0 : \ \tau = \tfrac{1}{2}, \ \vartheta = -\tfrac{1}{2} \\ &\varsigma < 0 : \tau = \tfrac{\varepsilon}{\pi}, \ \vartheta = -\tfrac{\varepsilon}{\pi} \end{aligned}$$

where ε is the same as that given in Eq. (49).

Inserting Eq. (47) into Eq. (63) and taking account into relation Eq. (52) produce the following expression:

$$\sum_{j=1}^{\infty} \tfrac{-L_{11}}{\sin(\pi\tau)} P_{j-1}^{(-\tau,-\vartheta)}(s) c_j = \tfrac{b}{2R} g(s), \ |s| < 1 \tag{65}$$

The function $g(s)$ can be expanded into a series of Jacobi Polynomials $P_j^{(-\tau,-\vartheta)}(\cdot)$

$$g(s) = s + 1 = P_1^{(-\tau,-\vartheta)}(s) + (1 + \tau) P_0^{(-\tau,-\vartheta)}(s) \tag{66}$$

Comparing the right-hand side of Eq. (65) and the left-hand side of Eq. (66), one can obtain nonzero coefficients as follows:

$$c_0 = \tfrac{b(1+\tau)}{2R} \sin(\pi\tau), \ c_1 = \tfrac{b}{2R} \sin(\pi\tau)$$

Thus, the solution of the stated problem can be obtained as

$$\varphi(\zeta) = \varpi(\zeta) \sum_{j=0}^{1} P_j^{(\tau,\vartheta)}(\zeta) = \frac{b(1 + 2\tau + \zeta)}{2R} \sin(\pi\tau)(1 - \zeta)^{\tau}(1 + \zeta)^{\vartheta}, \qquad |\zeta| < 1 \tag{67}$$

One edge of the present semi-parabolic stamp is unknown a priori, which can be determined by considering the equilibrium equation. Employing the orthogonality of the Jacobi Polynomials and relation (52) and substituting Eq. (67) into Eq. (64) yield

$$P = \frac{\pi \cdot \tau \cdot (1 + \tau)}{2R} b^2 \tag{68}$$

Eq. (68) reveals the relationship between the applied load and contact area.

The contact stress distribution in physical coordinates can be obtained by using Eqs. (31), (62), and (67)

$$\sigma_{zz}(x) = -\frac{b \sin(\pi\tau)}{R} \left(\frac{b - x}{x} \right)^{\tau} \left(\tau + \frac{x}{b} \right), \qquad 0 < x < b \tag{69}$$

In this case, the in-plane stress on the surface and in-plane electric displacement can be rewritten as

$$\sigma_{xx}(x,0)=\begin{cases} L_{21}p(x)+\frac{\mu_f}{\pi}\int\limits_0^b \frac{L_{22}}{\xi-x}p(\xi)\mathrm{d}\xi, & 0<x<b \\ \frac{\mu_f}{\pi}\int\limits_0^b \frac{L_{22}}{\xi-x}p(\xi)\mathrm{d}\xi, & x<0, x>b \end{cases} \tag{70}$$

$$D_x(x,0)=\begin{cases} L_{32}\mu_f p(x)+\frac{1}{\pi}\int\limits_0^b \frac{L_{31}}{\xi-x}p(\xi)\mathrm{d}\xi, & 0<x<b \\ \frac{1}{\pi}\int\limits_0^b \frac{L_{31}}{\xi-x}p(\xi)\mathrm{d}\xi, & x<0, x>b \end{cases} \tag{71}$$

Considering Eqs. (62) and (67), one can rewrite Eqs. (70) and (71) in the following closed-form (Guler and Erdogan [10]) based on Eq. (69):

$$\sigma_{xx}(x,0)=\frac{b}{R}\begin{cases} L_{21}\sin(\pi\tau)(\frac{b-x}{x})^{\tau}(\tau+\frac{x}{b})+\frac{b}{R}\frac{L_{22}\cdot\mu_f}{\pi}\sum\limits_{n=0}^{1}\mathrm{H}_n(x), & 0<x<b \\ \frac{b}{R}\frac{L_{22}\cdot\mu_f}{\pi}\sum\limits_{n=0}^{1}\mathrm{H}_n(x), & x<0, x>b \end{cases} \tag{72}$$

$$D_x(x,0)=\frac{b}{R}\begin{cases} L_{32}\cdot\mu_f\sin(\pi\tau)(\frac{b-x}{x})^{\tau}(\tau+\frac{x}{b})+\frac{b}{R}\frac{L_{31}}{\pi}\sum\limits_{n=0}^{1}\mathrm{H}_n(x), & 0<x<b \\ \frac{b}{R}\frac{L_{31}}{\pi}\sum\limits_{n=0}^{1}\mathrm{H}_n(x), & x<0, x>b \end{cases} \tag{73}$$

In Eqs. (72) and (73), $\mathrm{H}_n(x)(n=1,2)$ are

$$\mathrm{H}_0(x)=\frac{\pi}{\sin(\pi\tau)}\begin{cases} -\left(\frac{x-b}{x}\right)^{\tau}-1, & x<0 \\ \left(\frac{b-x}{x}\right)^{\tau}\cos(\pi\tau)-1, & 0<x<b \\ \left(\frac{x-b}{x}\right)^{\tau}-1, & x>b \end{cases}$$

$$H_1(x)=P_1^{(\tau,\vartheta)}\left(\frac{2x}{b}-1\right)H_0(x)+\frac{2\pi\tau}{\sin(\pi\tau)}$$

The mode I stress intensity factor at the edge ($x=0$) of the semi-parabolic stamp can be defined as

$$F_I(0)=\lim_{x\to 0}x^{\tau}p(x)=\frac{b^{\tau+1}\cdot\tau\cdot\sin(\pi\tau)}{R} \tag{74}$$

The friction coefficient $\mu_f=0$ leads to $\tau=-\vartheta=1/2$, then Eq. (74) becomes

$$F_I(0)=\frac{b^{\frac{3}{2}}}{2R}$$

7 Numerical results and discussions

For the foregoing analysis, the piezoelectric ceramic $PZT-5A$ (Vel and Batra [21]) is considered. The elastic constants are $c_{11}=99.201\times10^9\,\mathrm{N/m^2}$, $c_{13}=50.778\times10^9\,\mathrm{N/m^2}$, $c_{16}=99.201\times10^9\,\mathrm{N/m^2}$, $c_{33}=86.856\times10^9\,\mathrm{N/m^2}$, $c_{36}=50.778\times10^9\,\mathrm{N/m^2}$, $c_{44}=21.100\times10^9\,\mathrm{N/m^2}$, $c_{45}=54.016\times10^9\,\mathrm{N/m^2}$, $c_{55}=21.100\times10^9\,\mathrm{N/m^2}$, and $c_{66}=22.593\times10^9\,\mathrm{N/m^2}$. The nonzero piezoelectric constants are $e_{31}=-7.209\,\mathrm{C/m^2}$, $e_{33}=15.118\,\mathrm{C/m^2}$, $e_{36}=-7.029\,\mathrm{C/m^2}$, $e_{14}=12.322\,\mathrm{C/m^2}$ and $e_{15}=12.322\,\mathrm{C/m^2}$. The dielectric constants are $\in_{11}=15.3\times10^{-9}\,\mathrm{F/m}$, and $\in_{33}=15\times10^{-9}\,\mathrm{F/m}$. Here, since the coefficients c_{16}, c_{36}, c_{45}, e_{14}, and e_{36} could not be found in the open literature, the values are assumed.

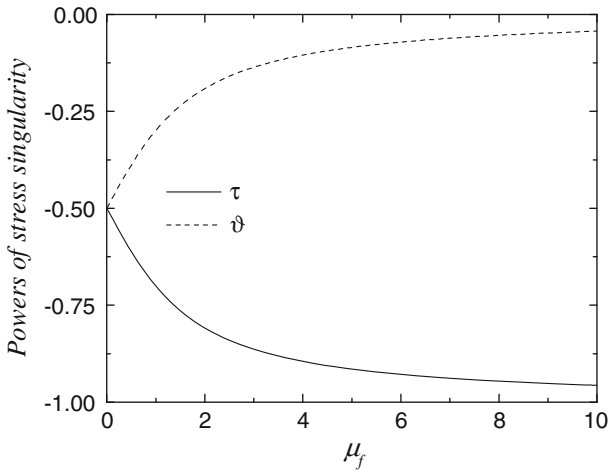

Fig. 2 The influence of the friction coefficient μ_f on the powers of stress singularity under a flat stamp

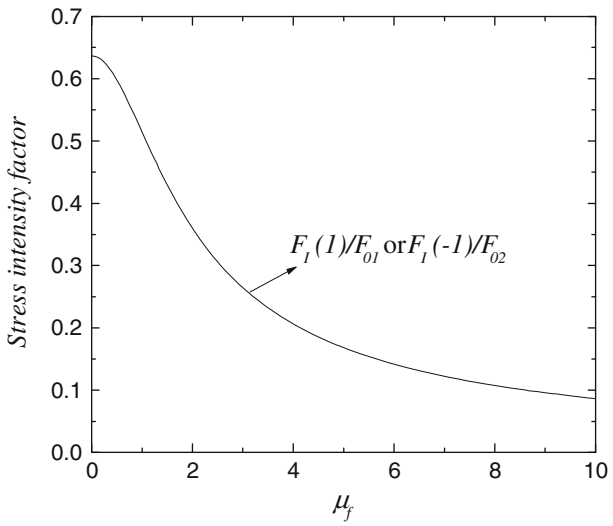

Fig. 3 The influence of the friction coefficient μ_f on the normalized stress intensity factor under a flat stamp

7.1 Contact behaviors under the frictional flat stamp

Figure 2 shows the variation of powers of stress singularity at the leading ($x = -a$) and the trailing ($x = a$) edges of the flat stamp with the friction coefficient μ_f changing. It can be seen $|\tau| > |\vartheta|$, which illustrates the singularity at the trailing edge of the flat stamp is stronger than that at the trailing edge. Therefore, greater stress concentration exists around the trailing edge. As $\mu_f \to 0$, $\vartheta \to -\frac{1}{2}$, and $\tau \to -\frac{1}{2}$ giving the traditional singularity at the flat stamp edges. The magnitude of τ increases and $\tau \to -1$ when μ_f becomes greater, while that of ϑ decreases and $\vartheta \to 0$.

Figure 3 shows the effects of the friction coefficient μ_f on the normalized stress intensity factors $F_I(1)/F_{01}$ and $F_I(-1)/F_{02}$, where $F_{01} = Pa^{\vartheta}$ and $F_{02} = Pa^{\tau}$. It can be seen that after the normalization, the normalized stress intensity factors are the same at the trailing edge and the leading edge. Figure 3 also demonstrates that the normalized stress intensity factors increase when the sliding contact interface between the stamp and piezoelectric materials becomes less frictional.

Figures 4, 5, and 6 show that the near-edge response that the severe stress concentrations exist around edges of the flat stamp. The magnitudes of all the surface stresses, that is, $\sigma_{zz}(x, 0)/\sigma_0$, $\sigma_{xz}(x, 0)/\sigma_0$, and $\sigma_{xx}(x, 0)/\sigma_0$ ($\sigma_0 = P/2a$) at the trailing edge are greater than those at the leading edge.

In addition, Fig. 4 depicts that the surface contact stress $\sigma_{zz}(x, 0)/\sigma_0$ is compressive beneath the stamp. The curve when the friction coefficient $\mu_f = 0$ denoting frictionless contact is symmetric, which shows the

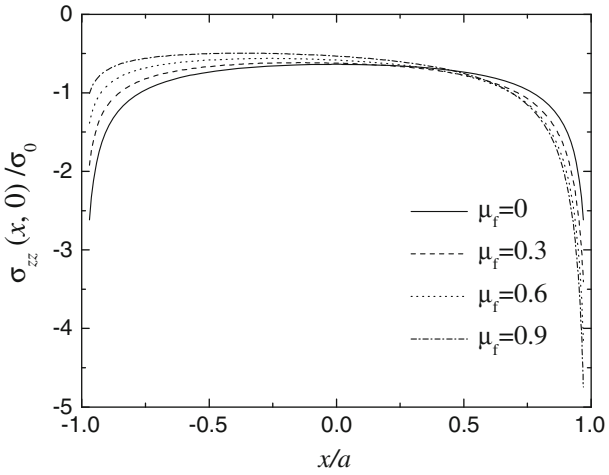

Fig. 4 The influence of the friction coefficient μ_f on the surface contact stress distribution $\sigma_{zz}(x,0)/\sigma_0$ under a flat stamp

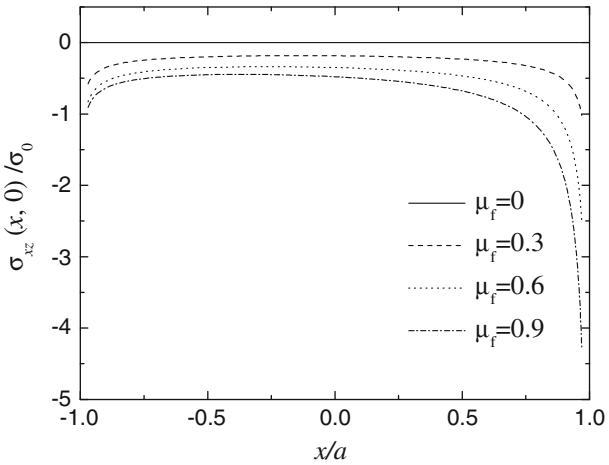

Fig. 5 The influence of the friction coefficient μ_f on the surface shear stress distribution $\sigma_{xz}(x,0)/\sigma_0$ under a flat stamp

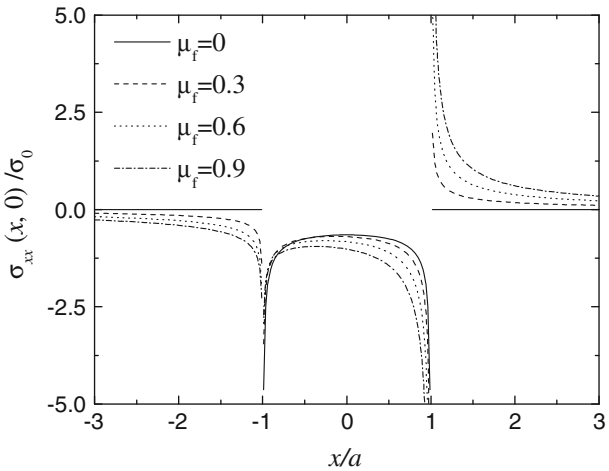

Fig. 6 The influence of the friction coefficient μ_f on the surface in-plane distribution $\sigma_{xx}(x,0)/\sigma_0$ under a flat stamp

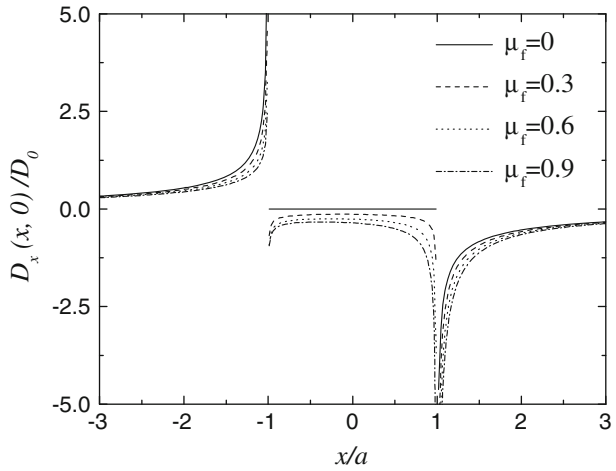

Fig. 7 The influence of the friction coefficient μ_f on the surface electric displacement distribution $D_x(x, 0)/D_0$ under a flat stamp

validity of the present program. With the sliding contact interface between the stamp and piezoelectric materials becoming more frictional, the surface contact stress intensifies at the trailing edge of the flat stamp, while becomes weaker at the leading edge of the flat stamp.

Figure 5 also illustrates the surface shear stress $\sigma_{xz}(x, 0)/\sigma_0$ is compressive when $\mu_f > 0$. The magnitude of $\sigma_{xz}(x, 0)/\sigma_0$ enhances with the increasing of friction coefficient.

Figure 6 also depicts the in-plane surface stress $\sigma_{xx}(x, 0)/\sigma_0$ is unbounded and discontinuous at both the trailing edge and the leading edge of the flat stamp. The in-plane surface stress intensifies at the trailing edge of the flat stamp, while becomes weaker at the leading edge of the flat stamp with the increasing of friction coefficient. The in-plane surface stress becomes more compressive behind the leading edge $(x < -a)$, while tends to more tensile before the trailing edge $(x > a)$ with the contact becoming more frictional.

Figure 7 shows the distribution of the surface electric displacement $D_x(x, 0)/D_0$ under a flat stamp, where the magnitude of D_0 is $P/2a$. It can be seen that the surface electric displacement is unbounded and discontinuous at both edges of the flat stamp. The surface electric displacement is positive when $x < -a$, while becomes negative when either $|x| < a$ or $x > a$. As the contact becomes more frictional, the magnitude of the surface electric displacement decreases when $x < -a$, while increases when either $|x| < a$ or $x > a$.

7.2 Contact behaviors under the frictional semi-parabolic stamp

Figure 8 shows the variation of powers of stress singularity at the edges of the semi-parabolic stamp with the friction coefficient μ_f changing. It can be seen that τ is positive and ϑ is negative due to the physics of the problem. As $\mu_f \to 0$, the singularities $\tau \to \frac{1}{2}$ and $\vartheta \to -\frac{1}{2}$. With the friction coefficient μ_f becoming greater, the singularities $\tau \to 0$ and $\vartheta \to 0$.

Figures 9, 10, 11, and 12 show the influences of the friction coefficient μ_f on various distributions of surface stresses $\sigma_{zz}(x, 0)/\sigma_0$, $\sigma_{xz}(x, 0)/\sigma_0$, and $\sigma_{xx}(x, 0)/\sigma_0$ $(\sigma_0 = P/R)$, and the distribution of the surface electric displacement $D_x(x, 0)/D_0$ (the magnitude of D_0 is P/R) under a semi-parabolic stamp. It can be seen that the contact region becomes wider with the sliding contact interface between the stamp and piezoelectric materials becoming more frictional.

In addition, Figures 9 and 10 demonstrate that the surface contact stress $\sigma_{zz}(x, 0)/\sigma_0$ and surface shear stress $\sigma_{xz}(x, 0)/\sigma_0$ are unbounded at the leading edge $(x = 0)$ and are equal to zero at another edge $(x = b)$. With the friction coefficient μ_f becoming greater, the surface contact stress $\sigma_{zz}(x, 0)/\sigma_0$ at the leading edge weakens, while surface shear stress $\sigma_{xz}(x, 0)/\sigma_0$ intensifies.

Figure 11 shows the surface in-plane stress $\sigma_{xx}(x, 0)/\sigma_0$ is unbounded and discontinuous at the leading edge $(x = 0)$. There is a tensile spike at another edge $(x = b)$ for the surface in-plane stress $\sigma_{xx}(x, 0)/\sigma_0$. As the friction coefficient μ_f increases, the surface in-plane stress $\sigma_{xx}(x, 0)/\sigma_0$ at the leading edge weakens.

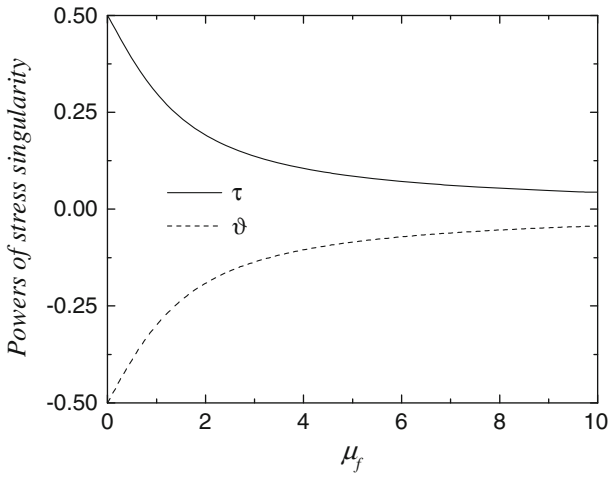

Fig. 8 The influence of the friction coefficient μ_f on the powers of stress singularity under a semi-parabolic stamp

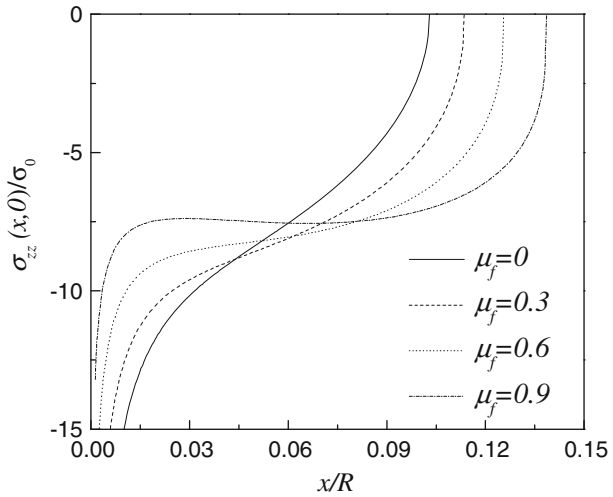

Fig. 9 The influence of the friction coefficient μ_f on the surface contact stress distribution $\sigma_{zz}(x, 0)/\sigma_0$ under a semi-parabolic stamp

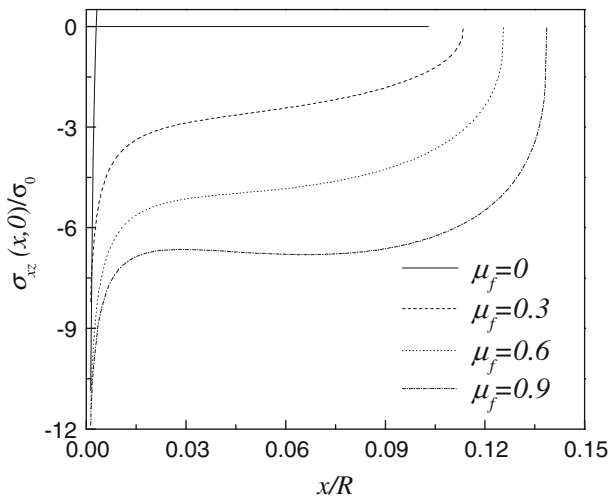

Fig. 10 The influence of the friction coefficient μ_f on the surface shear stress distribution $\sigma_{xz}(x, 0)/\sigma_0$ under a semi-parabolic stamp

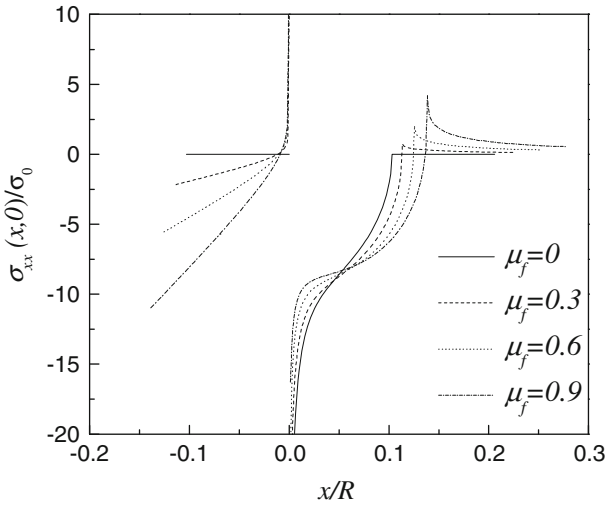

Fig. 11 The influence of the friction coefficient μ_f on the surface in-plane distribution $\sigma_{xx}(x,0)/\sigma_0$ under a semi-parabolic stamp

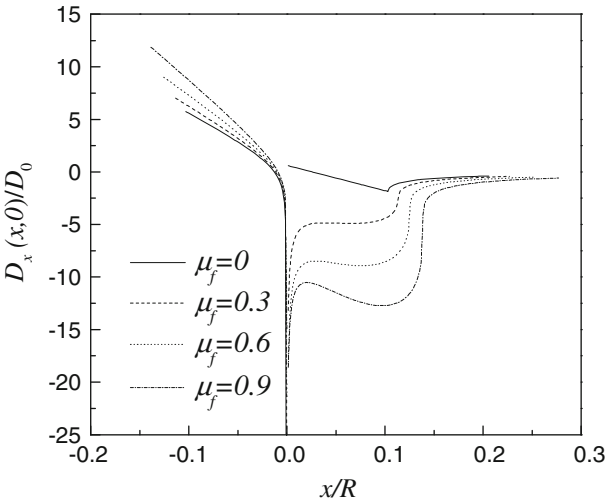

Fig. 12 The influence of the friction coefficient μ_f on the surface electric displacement distribution $D_x(x,0)/D_0$ under a semi-parabolic stamp

Figure 12 depicts the surface electric displacement $D_x(x,0)/D_0$ is unbounded and discontinuous at the leading edge ($x=0$). The surface electric displacement $D_x(x,0)/D_0$ at the leading edge intensifies with enhancing the friction coefficient μ_f.

8 Conclusions

The present paper conducts an exact analysis of frictional contact of anisotropic piezoelectric materials under a rigid stamp, which possesses a flat or semi-parabolic foundation. There are three cases of eigenvalue distribution for the commercially available anisotropic piezoelectric materials. For each case, fundamental solutions that can lead to real values of physical quantities are given. The stated problems can be reduced into a singular integral equation of the second kind, which can be solved exactly. For either a flat stamp or a semi-parabolic stamp, explicit expressions of various surface stresses and electric displacement are derived. Moreover, relationships between the applied load and contact area are obtained and stress intensity factors at stamp edges are given. Finally, figures are plotted to clearly illustrate the effects of the friction coefficient on various surface stresses and electric displacement.

The present study could provide a scientific basis for the theoretical and experimental test of contact behaviors of anisotropic piezoelectric materials.

Acknowledgments The authors would like to thank the anonymous reviewers for their helpful suggestions to improve this paper. This work was supported by the National Natural Science Foundation of China (10962008, 51061015, and 61063020).

Appendix

1. *The matrix* $G = (g_{mn})$ $(m, n = 1, 2, 3, 4)$ *appearing in Eq. (16)*

$$
\begin{aligned}
&g_{mn} = g_{nm}, \quad m, n = 1, 2, 3, 4\\
&g_{11} = c_{55}\eta^2 - c_{11}, \quad g_{12} = c_{45}\eta^2 - c_{16}, \quad g_{13} = -i \cdot \mathrm{sgn}(\omega) \cdot g^0_{13}, \quad g_{14} = -i \cdot \mathrm{sgn}(\omega) \cdot g^0_{14}\\
&g_{22} = c_{44}\eta^2 - c_{66}, \quad g_{23} = -i \cdot \mathrm{sgn}(\omega) \cdot g^0_{23}, \quad g_{24} = -i \cdot \mathrm{sgn}(\omega) \cdot g^0_{24}\\
&g_{33} = c_{33}\eta^2 - c_{55}, \quad g_{34} = e_{33}\eta^2 - e_{15}, \quad g_{44} = \in_{33} \eta^2 - \in_{11}
\end{aligned}
$$

where $\mathrm{sgn}(\cdot)$ denotes the sign function, and g^0_{13}, g^0_{14}, g^0_{23} and g^0_{24} are given as

$$
g^0_{13} = (c_{13} + c_{55})\,\eta, \quad g^0_{14} = (e_{31} + e_{15})\,\eta, \quad g^0_{23} = (c_{36} + c_{45})\,\eta, \quad g^0_{24} = (e_{36} + e_{14})\,\eta
$$

Here

$$
g_{mn} = g_{nm}, g^0_{mn} = g^0_{nm}
$$

2. *Expressions of* $f_0(\eta)$, $f_D(\eta)$, $g_0(\eta)$ *and* $h_0(\eta)$ *appearing in Eq. (23)*

$$
\begin{aligned}
f_0(\eta) &= g_{11}g^0_{23}g_{34} - g_{11}g^0_{24}g_{33} - g_{21}g^0_{13}g_{34} + g_{21}g^0_{14}g_{33} - g^0_{31}g^0_{13}g^0_{24} + g^0_{31}g^0_{14}g^0_{23}\\
f_D(\eta) &= -g_{12}g^0_{23}g_{34} + g_{12}g^0_{24}g_{33} + g_{22}g^0_{13}g_{34} - g_{22}g^0_{14}g_{33} + g^0_{32}g^0_{13}g^0_{24} - g^0_{32}g^0_{14}g^0_{23}\\
g_0(\eta) &= -g_{12}g_{21}g_{34} - g_{12}g^0_{24}g^0_{31} + g_{22}g_{11}g_{34} + g_{22}g^0_{14}g^0_{31} + g^0_{32}g_{11}g^0_{24} - g^0_{32}g^0_{14}g_{21}\\
h_0(\eta) &= g_{12}g_{21}g^0_{31} + g_{12}g_{21}g_{33} - g_{22}g^0_{13}g^0_{31} - g_{22}g_{11}g_{33} + g^0_{32}g^0_{13}g_{21} - g^0_{32}g_{11}g^0_{23}
\end{aligned}
$$

3. *Expressions of* $\Omega^{(s)}_{mj}(\omega, z)$ $(m = 0, 1, 2, 3, j = 1, 2, 3, 4)$ and $\Omega^{(e)}_{nj}(\omega, z)$ $(n = 0, 1, j = 1, 2, 3, 4)$ *appearing in Eqs. (28) and (29)*
For Case A

$$
\begin{aligned}
\Omega^{(s)}_{0j}(\omega, z) &= -i \cdot \mathrm{sgn}(\omega)\left[c_{11} + c_{16}f(o_j) + c_{13}o_j g(o_j) + e_{31}o_j h(o_j)\right]e^{|\omega|o_j z}, \quad j = 1, 2, 3, 4\\
\Omega^{(s)}_{1j}(\omega, z) &= -i \cdot \mathrm{sgn}(\omega)\left[c_{13} + c_{36}f(o_j) + c_{33}o_j g(o_j) + e_{33}o_j h(o_j)\right]e^{|\omega|o_j z}, \quad j = 1, 2, 3, 4\\
\Omega^{(s)}_{2j}(\omega, z) &= \left\{c_{55}\left[o_j - g(o_j)\right] + c_{45}o_j f(o_j) - e_{15}h(o_j)\right\}e^{|\omega|o_j z}, \quad j = 1, 2, 3, 4\\
\Omega^{(s)}_{3j}(\omega, z) &= \left\{c_{45}\left[o_j - g(o_j)\right] + c_{44}o_j f(o_j) - e_{14}h(o_j)\right\}e^{|\omega|o_j z}, \quad j = 1, 2, 3, 4\\
\Omega^{(e)}_{0j}(\omega, z) &= \left\{e_{15}\left[o_j - g(o_j)\right] + e_{14}o_j f(o_j) + \in_{11} h(o_j)\right\}e^{|\omega|o_j z}, \quad j = 1, 2, 3, 4\\
\Omega^{(e)}_{1j}(\omega, z) &= -i \cdot \mathrm{sgn}(\omega)\left[e_{31} + e_{36}f(o_j) + e_{33}o_j g(o_j) - \in_{33} o_j h(o_j)\right]e^{|\omega|o_j z}, \quad j = 1, 2, 3, 4
\end{aligned}
$$

For Case B

$$
\begin{aligned}
\Omega^{(s)}_{0j}(\omega, z) &= -i \cdot \mathrm{sgn}(\omega)\left[c_{11} + c_{16}f(o_j) + c_{13}o_j g(o_j) + e_{31}o_j h(o_j)\right]e^{|\omega|o_j z}, \quad j = 1, 2\\
\Omega^{(s)}_{03}(\omega, z) &= -i \cdot \mathrm{sgn}(\omega)\{[c_{11} + c_{16}\Gamma_V + c_{13}\,(o_3\Gamma_W - \sigma_3\Delta_W)\\
&\quad + e_{31}\,(o_3\Gamma_\Phi - \sigma_3\Delta_\Phi)]\cos(|\omega|\,\sigma_3 z) - [c_{16}\Delta_V + c_{13}\,(o_3\Delta_W + \sigma_3\Gamma_W)\\
&\quad + e_{31}\,(o_3\Delta_\Phi + \sigma_3\Gamma_\Phi)]\sin(|\omega|\,\sigma_3 z)\}\,e^{|\omega|o_3 z}\\
\Omega^{(s)}_{04}(\omega, z) &= -i \cdot \mathrm{sgn}(\omega)\{[c_{16}\Delta_V + c_{13}\,(o_3\Delta_W + \sigma_3\Gamma_W)
\end{aligned}
$$

$$
\begin{aligned}
&+e_{31}\left(o_3\Delta_\Phi+\sigma_3\Gamma_\Phi\right)]\cos(|\omega|\,\sigma_3 z)+[c_{11}+c_{16}\Gamma_V+c_{13}\left(o_3\Gamma_W-\sigma_3\Delta_W\right)\\
&+e_{31}\left(o_3\Gamma_\Phi-\sigma_3\Delta_\Phi\right)]\sin(|\omega|\,\sigma_3 z)\}\,e^{|\omega|o_3 z}\\
\Omega_{1j}^{(s)}(\omega,z)&=-i\cdot\mathrm{sgn}(\omega)\left[c_{13}+c_{36}f(o_j)+c_{33}o_j g(o_j)+e_{33}o_j h(o_j)\right]e^{|\omega|o_j z},\quad j=1,2\\
\Omega_{13}^{(s)}(\omega,z)&=-i\cdot\mathrm{sgn}(\omega)\,\{[c_{13}+c_{36}\Gamma_V+c_{33}\left(o_3\Gamma_W-\sigma_3\Delta_W\right)\\
&+e_{33}\left(o_3\Gamma_\Phi-\sigma_3\Delta_\Phi\right)]\cos(|\omega|\,\sigma_3 z)-[c_{36}\Delta_V+c_{33}\left(o_3\Delta_W+\sigma_3\Gamma_W\right)\\
&+e_{33}\left(o_3\Delta_\Phi+\sigma_3\Gamma_\Phi\right)]\sin(|\omega|\,\sigma_3 z)\}\,e^{|\omega|o_3 z}\\
\Omega_{14}^{(s)}(\omega,z)&=-i\cdot\mathrm{sgn}(\omega)\,\{[c_{36}\Delta_V+c_{33}\left(o_3\Delta_W+\sigma_3\Gamma_W\right)\\
&+e_{33}\left(o_3\Delta_\Phi+\sigma_3\Gamma_\Phi\right)]\cos(|\omega|\,\sigma_3 z)+[c_{13}+c_{36}\Gamma_V+c_{33}\left(o_3\Gamma_W-\sigma_3\Delta_W\right)\\
&+e_{33}\left(o_3\Gamma_\Phi-\sigma_3\Delta_\Phi\right)]\sin(|\omega|\,\sigma_3 z)\}\,e^{|\omega|o_3 z}\\
\Omega_{2j}^{(s)}(\omega,z)&=\left\{c_{55}\left[o_j-g(o_j)\right]+c_{45}o_j f(o_j)-e_{15}h(o_j)\right\}e^{|\omega|o_j z},\quad j=1,2\\
\Omega_{23}^{(s)}(\omega,z)&=\{[c_{55}\left(o_3-\Gamma_W\right)+c_{45}\left(o_3\Gamma_V-\sigma_3\Delta_V\right)-e_{15}\Gamma_\Phi]\cos(|\omega|\,\sigma_3 z)\\
&+[c_{55}\left(-\sigma_3+\Delta_W\right)-c_{45}\left(\sigma_3\Gamma_V+o_3\Delta_V\right)+e_{15}\Delta_\Phi]\sin(|\omega|\,\sigma_3 z)\}\,e^{|\omega|o_3 z}\\
\Omega_{24}^{(s)}(\omega,z)&=\{[c_{55}\left(\sigma_3-\Delta_W\right)+c_{45}\left(\sigma_3\Gamma_V+o_3\Delta_V\right)-e_{15}\Delta_\Phi]\cos(|\omega|\,\sigma_3 z)\\
&+[c_{55}\left(o_3-\Gamma_W\right)+c_{45}\left(o_3\Gamma_V-\sigma_3\Delta_V\right)-e_{15}\Gamma_\Phi]\sin(|\omega|\,\sigma_3 z)\}\,e^{|\omega|o_3 z}\\
\Omega_{3j}^{(s)}(\omega,z)&=\left\{c_{45}\left[o_j-g(o_j)\right]+c_{44}o_j f(o_j)-e_{14}h(o_j)\right\}e^{|\omega|o_j z},\quad j=1,2\\
\Omega_{33}^{(s)}(\omega,z)&=\{[c_{45}\left(o_3-\Gamma_W\right)+c_{44}\left(o_3\Gamma_V-\sigma_3\Delta_V\right)-e_{14}\Gamma_\Phi]\cos(|\omega|\,\sigma_3 z)\\
&+[c_{45}\left(-\sigma_3+\Delta_W\right)-c_{44}\left(\sigma_3\Gamma_V+o_3\Delta_V\right)+e_{14}\Delta_\Phi]\sin(|\omega|\,\sigma_3 z)\}\,e^{|\omega|o_3 z}\\
\Omega_{34}^{(s)}(\omega,z)&=\{[c_{45}\left(\sigma_3-\Delta_W\right)+c_{44}\left(\sigma_3\Gamma_V+o_3\Delta_V\right)-e_{14}\Delta_\Phi]\cos(|\omega|\,\sigma_3 z)\\
&+[c_{45}\left(o_3-\Gamma_W\right)+c_{44}\left(o_3\Gamma_V-\sigma_3\Delta_V\right)-e_{14}\Gamma_\Phi]\sin(|\omega|\,\sigma_3 z)\}\,e^{|\omega|o_3 z}\\
\Omega_{0j}^{(e)}(\omega,z)&=\left\{e_{15}\left[o_j-g(o_j)\right]+e_{14}o_j f(o_j)+\in_{11}h(o_j)\right\}e^{|\omega|o_j z},\qquad j=1,2\\
\Omega_{03}^{(e)}(\omega,z)&=\{[e_{15}\left(o_3-\Gamma_W\right)+e_{14}\left(o_3\Gamma_V-\sigma_3\Delta_V\right)+\in_{11}\Gamma_\Phi]\cos(|\omega|\,\sigma_3 z)\\
&+[e_{15}\left(-\sigma_3+\Delta_W\right)-e_{14}\left(\sigma_3\Gamma_V+o_3\Delta_V\right)-\in_{11}\Delta_\Phi]\sin(|\omega|\,\sigma_3 z)\}\,e^{|\omega|o_3 z}\\
\Omega_{04}^{(e)}(\omega,z)&=\{[e_{15}\left(\sigma_3-\Delta_W\right)+e_{14}\left(\sigma_3\Gamma_V+o_3\Delta_V\right)+\in_{11}\Delta_\Phi]\cos(|\omega|\,\sigma_3 z)\\
&+[e_{15}\left(o_3-\Gamma_W\right)+e_{14}\left(o_3\Gamma_V-\sigma_3\Delta_V\right)+\in_{11}\Gamma_\Phi]\sin(|\omega|\,\sigma_3 z)\}\,e^{|\omega|o_3 z}\\
\Omega_{1j}^{(e)}(\omega,z)&=-i\cdot\mathrm{sgn}(\omega)\left[e_{31}+e_{36}f(o_j)+e_{33}o_j g(o_j)-\in_{33}o_j h(o_j)\right]e^{|\omega|o_j z},\quad j=1,2\\
\Omega_{13}^{(e)}(\omega,z)&=-i\cdot\mathrm{sgn}(\omega)\,\{[e_{31}+e_{36}\Gamma_V+e_{33}\left(o_3\Gamma_W-\sigma_3\Delta_W\right)\\
&-\in_{33}\left(o_3\Gamma_\Phi-\sigma_3\Delta_\Phi\right)]\cos(|\omega|\,\sigma_3 z)-[e_{36}\Delta_V+e_{33}\left(o_3\Delta_W+\sigma_3\Gamma_W\right)\\
&-\in_{33}\left(o_3\Delta_\Phi+\sigma_3\Gamma_\Phi\right)]\sin(|\omega|\,\sigma_3 z)\}\,e^{|\omega|o_3 z}\\
\Omega_{14}^{(e)}(\omega,z)&=-i\cdot\mathrm{sgn}(\omega)\,\{[[e_{36}\Delta_V+e_{33}\left(o_3\Delta_W+\sigma_3\Gamma_W\right)\\
&-\in_{33}\left(o_3\Delta_\Phi+\sigma_3\Gamma_\Phi\right)]\cos(|\omega|\,\sigma_3 z)+[e_{31}+e_{36}\Gamma_V+e_{33}\left(o_3\Gamma_W-\sigma_3\Delta_W\right)\\
&-\in_{33}\left(o_3\Gamma_\Phi-\sigma_3\Delta_\Phi\right)]\sin(|\omega|\,\sigma_3 z)\}\,e^{|\omega|o_3 z}
\end{aligned}
$$

For Case C

$$
\begin{aligned}
\Omega_{01}^{(s)}(\omega,z)&=-i\cdot\mathrm{sgn}(\omega)\left\{\left[c_{11}+c_{16}\Gamma_V^{(1)}+c_{13}\left(o_1\Gamma_W^{(1)}-\sigma_1\Delta_W^{(1)}\right)\right.\right.\\
&\left.+e_{31}\left(o_1\Gamma_\Phi^{(1)}-\sigma_1\Delta_\Phi^{(1)}\right)\right]\cos(|\omega|\,\sigma_1 z)-\left[c_{16}\Delta_V^{(1)}+c_{13}\left(o_1\Delta_W^{(1)}+\sigma_1\Gamma_W^{(1)}\right)\right.\\
&\left.\left.+e_{31}\left(o_1\Delta_\Phi^{(1)}+\sigma_1\Gamma_\Phi^{(1)}\right)\right]\sin(|\omega|\,\sigma_1 z)\right\}e^{|\omega|o_1 z}\\
\Omega_{02}^{(s)}(\omega,z)&=-i\cdot\mathrm{sgn}(\omega)\left\{\left[c_{16}\Delta_V^{(1)}+c_{13}\left(o_1\Delta_W^{(1)}+\sigma_1\Gamma_W^{(1)}\right)\right.\right.\\
&\left.+e_{31}\left(o_1\Delta_\Phi^{(1)}+\sigma_1\Gamma_\Phi^{(1)}\right)\right]\cos(|\omega|\,\sigma_1 z)+\left[c_{11}+c_{16}\Gamma_V^{(1)}+c_{13}\left(o_1\Gamma_W^{(1)}-\sigma_1\Delta_W^{(1)}\right)\right.
\end{aligned}
$$

$$
\begin{aligned}
&+e_{31}\left(o_1\Gamma_{\Phi}^{(1)}-\sigma_1\Delta_{\Phi}^{(1)}\right)\Big]\sin(|\omega|\,\sigma_1 z)\Big\}\,e^{|\omega|o_1 z}\\
\Omega_{03}^{(s)}(\omega,z)=&-i\cdot\operatorname{sgn}(\omega)\Big\{\Big[c_{11}+c_{16}\Gamma_V^{(2)}+c_{13}\left(o_3\Gamma_W^{(2)}-\sigma_3\Delta_W^{(2)}\right)\\
&+e_{31}\left(o_3\Gamma_{\Phi}^{(2)}-\sigma_3\Delta_{\Phi}^{(2)}\right)\Big]\cos(|\omega|\,\sigma_3 z)-\Big[c_{16}\Delta_V^{(2)}+c_{13}\left(o_3\Delta_W^{(2)}+\sigma_3\Gamma_W^{(2)}\right)\\
&+e_{31}\left(o_3\Delta_{\Phi}^{(2)}+\sigma_3\Gamma_{\Phi}^{(2)}\right)\Big]\sin(|\omega|\,\sigma_3 z)\Big\}\,e^{|\omega|o_3 z}\\
\Omega_{04}^{(s)}(\omega,z)=&-i\cdot\operatorname{sgn}(\omega)\Big\{\Big[c_{16}\Delta_V^{(2)}+c_{13}\left(o_3\Delta_W^{(2)}+\sigma_3\Gamma_W^{(2)}\right)\\
&+e_{31}\left(o_3\Delta_{\Phi}^{(2)}+\sigma_3\Gamma_{\Phi}^{(2)}\right)\Big]\cos(|\omega|\,\sigma_3 z)+\Big[c_{11}+c_{16}\Gamma_V^{(2)}+c_{13}\left(o_3\Gamma_W^{(2)}-\sigma_3\Delta_W^{(2)}\right)\\
&+e_{31}\left(o_3\Gamma_{\Phi}^{(2)}-\sigma_3\Delta_{\Phi}^{(2)}\right)\Big]\sin(|\omega|\,\sigma_3 z)\Big\}\,e^{|\omega|o_3 z}\\
\Omega_{11}^{(s)}(\omega,z)=&-i\cdot\operatorname{sgn}(\omega)\Big\{\Big[c_{13}+c_{36}\Gamma_V^{(1)}+c_{33}\left(o_1\Gamma_W^{(1)}-\sigma_1\Delta_W^{(1)}\right)\\
&+e_{33}\left(o_1\Gamma_{\Phi}^{(1)}-\sigma_1\Delta_{\Phi}^{(1)}\right)\Big]\cos(|\omega|\,\sigma_1 z)-\Big[c_{36}\Delta_V^{(1)}+c_{33}\left(o_1\Delta_W^{(1)}+\sigma_1\Gamma_W^{(1)}\right)\\
&+e_{33}\left(o_1\Delta_{\Phi}^{(1)}+\sigma_1\Gamma_{\Phi}^{(1)}\right)\Big]\sin(|\omega|\,\sigma_1 z)\Big\}\,e^{|\omega|o_1 z}\\
\Omega_{12}^{(s)}(\omega,z)=&-i\cdot\operatorname{sgn}(\omega)\Big\{\Big[c_{36}\Delta_V^{(1)}+c_{33}\left(o_1\Delta_W^{(1)}+\sigma_1\Gamma_W^{(1)}\right)\\
&+e_{33}\left(o_1\Delta_{\Phi}^{(1)}+\sigma_1\Gamma_{\Phi}^{(1)}\right)\Big]\cos(|\omega|\,\sigma_1 z)+\Big[c_{13}+c_{36}\Gamma_V^{(1)}+c_{33}\left(o_1\Gamma_W^{(1)}-\sigma_1\Delta_W^{(1)}\right)\\
&+e_{33}\left(o_1\Gamma_{\Phi}^{(1)}-\sigma_1\Delta_{\Phi}^{(1)}\right)\Big]\sin(|\omega|\,\sigma_1 z)\Big\}\,e^{|\omega|o_1 z}\\
\Omega_{13}^{(s)}(\omega,z)=&-i\cdot\operatorname{sgn}(\omega)\Big\{\Big[c_{13}+c_{36}\Gamma_V^{(2)}+c_{33}\left(o_3\Gamma_W^{(2)}-\sigma_3\Delta_W^{(2)}\right)\\
&+e_{33}\left(o_3\Gamma_{\Phi}^{(2)}-\sigma_3\Delta_{\Phi}^{(2)}\right)\Big]\cos(|\omega|\,\sigma_3 z)-\Big[c_{36}\Delta_V^{(2)}+c_{33}\left(o_3\Delta_W^{(2)}+\sigma_3\Gamma_W^{(2)}\right)\\
&+e_{33}\left(o_3\Delta_{\Phi}^{(2)}+\sigma_3\Gamma_{\Phi}^{(2)}\right)\Big]\sin(|\omega|\,\sigma_3 z)\Big\}\,e^{|\omega|o_3 z}\\
\Omega_{14}^{(s)}(\omega,z)=&-i\cdot\operatorname{sgn}(\omega)\Big\{\Big[c_{36}\Delta_V^{(2)}+c_{33}\left(o_3\Delta_W^{(2)}+\sigma_3\Gamma_W^{(2)}\right)\\
&+e_{33}\left(o_3\Delta_{\Phi}^{(2)}+\sigma_3\Gamma_{\Phi}^{(2)}\right)\Big]\cos(|\omega|\,\sigma_3 z)+\Big[c_{13}+c_{36}\Gamma_V^{(2)}+c_{33}\left(o_3\Gamma_W^{(2)}-\sigma_3\Delta_W^{(2)}\right)\\
&+e_{33}\left(o_3\Gamma_{\Phi}^{(2)}-\sigma_3\Delta_{\Phi}^{(2)}\right)\Big]\sin(|\omega|\,\sigma_3 z)\Big\}\,e^{|\omega|o_3 z}\\
\Omega_{21}^{(s)}(\omega,z)=&\Big\{\Big[c_{55}\left(o_1-\Gamma_W^{(1)}\right)+c_{45}\left(o_1\Gamma_V^{(1)}-\sigma_1\Delta_V^{(1)}\right)-e_{15}\Gamma_{\Phi}^{(1)}\Big]\cos(|\omega|\,\sigma_1 z)\\
&+\Big[c_{55}\left(-\sigma_1+\Delta_W^{(1)}\right)-c_{45}\left(\sigma_1\Gamma_V^{(1)}+o_1\Delta_V^{(1)}\right)+e_{15}\Delta_{\Phi}^{(1)}\Big]\sin(|\omega|\,\sigma_1 z)\Big\}\,e^{|\omega|o_1 z}\\
\Omega_{22}^{(s)}(\omega,z)=&\Big\{\Big[c_{55}\left(\sigma_1-\Delta_W^{(1)}\right)+c_{45}\left(\sigma_1\Gamma_V^{(1)}+o_1\Delta_V^{(1)}\right)-e_{15}\Delta_{\Phi}^{(1)}\Big]\cos(|\omega|\,\sigma_1 z)\\
&+\Big[c_{55}\left(o_1-\Gamma_W^{(1)}\right)+c_{45}\left(o_1\Gamma_V^{(1)}-\sigma_1\Delta_V^{(1)}\right)-e_{15}\Gamma_{\Phi}^{(1)}\Big]\sin(|\omega|\,\sigma_1 z)\Big\}\,e^{|\omega|o_1 z}\\
\Omega_{23}^{(s)}(\omega,z)=&\Big\{\Big[c_{55}\left(o_3-\Gamma_W^{(2)}\right)+c_{45}\left(o_3\Gamma_V^{(2)}-\sigma_3\Delta_V^{(2)}\right)-e_{15}\Gamma_{\Phi}^{(2)}\Big]\cos(|\omega|\,\sigma_3 z)\\
&+\Big[c_{55}\left(-\sigma_3+\Delta_W^{(2)}\right)-c_{45}\left(\sigma_3\Gamma_V^{(2)}+o_3\Delta_V^{(2)}\right)+e_{15}\Delta_{\Phi}^{(2)}\Big]\sin(|\omega|\,\sigma_3 z)\Big\}\,e^{|\omega|o_3 z}\\
\Omega_{24}^{(s)}(\omega,z)=&\Big\{\Big[c_{55}\left(\sigma_3-\Delta_W^{(2)}\right)+c_{45}\left(\sigma_3\Gamma_V^{(2)}+o_3\Delta_V^{(2)}\right)-e_{15}\Delta_{\Phi}^{(2)}\Big]\cos(|\omega|\,\sigma_3 z)\\
&+\Big[c_{55}\left(o_3-\Gamma_W^{(2)}\right)+c_{45}\left(o_3\Gamma_V^{(2)}-\sigma_3\Delta_V^{(2)}\right)-e_{15}\Gamma_{\Phi}^{(2)}\Big]\sin(|\omega|\,\sigma_3 z)\Big\}\,e^{|\omega|o_3 z}\\
\Omega_{31}^{(s)}(\omega,z)=&\Big\{\Big[c_{45}\left(o_1-\Gamma_W^{(1)}\right)+c_{44}\left(o_1\Gamma_V^{(1)}-\sigma_1\Delta_V^{(1)}\right)-e_{14}\Gamma_{\Phi}^{(1)}\Big]\cos(|\omega|\,\sigma_1 z)\\
&+\Big[c_{45}\left(-\sigma_1+\Delta_W^{(1)}\right)-c_{44}\left(\sigma_1\Gamma_V^{(1)}+o_1\Delta_V^{(1)}\right)+e_{14}\Delta_{\Phi}^{(1)}\Big]\sin(|\omega|\,\sigma_1 z)\Big\}\,e^{|\omega|o_1 z}
\end{aligned}
$$

$$\Omega_{32}^{(s)}(\omega,z)=\left\{\left[c_{45}\left(\sigma_1-\Delta_W^{(1)}\right)+c_{44}\left(\sigma_1\Gamma_V^{(1)}+o_1\Delta_V^{(1)}\right)-e_{14}\Delta_\Phi^{(1)}\right]\cos(|\omega|\,\sigma_1 z)\right.$$
$$\left.+\left[c_{45}\left(o_1-\Gamma_W^{(1)}\right)+c_{44}\left(o_1\Gamma_V^{(1)}-\sigma_1\Delta_V^{(1)}\right)-e_{14}\Gamma_\Phi^{(1)}\right]\sin(|\omega|\,\sigma_1 z)\right\}e^{|\omega|o_1 z}$$
$$\Omega_{33}^{(s)}(\omega,z)=\left\{\left[c_{45}\left(o_3-\Gamma_W^{(2)}\right)+c_{44}\left(o_3\Gamma_V^{(2)}-\sigma_3\Delta_V^{(2)}\right)-e_{14}\Gamma_\Phi^{(2)}\right]\cos(|\omega|\,\sigma_3 z)\right.$$
$$\left.+\left[c_{45}\left(-\sigma_3+\Delta_W^{(2)}\right)-c_{44}\left(\sigma_3\Gamma_V^{(2)}+o_3\Delta_V^{(2)}\right)+e_{14}\Delta_\Phi^{(2)}\right]\sin(|\omega|\,\sigma_3 z)\right\}e^{|\omega|o_3 z}$$
$$\Omega_{34}^{(s)}(\omega,z)=\left\{\left[c_{45}\left(\sigma_3-\Delta_W^{(2)}\right)+c_{44}\left(\sigma_3\Gamma_V^{(2)}+o_3\Delta_V^{(2)}\right)-e_{14}\Delta_\Phi^{(2)}\right]\cos(|\omega|\,\sigma_3 z)\right.$$
$$\left.+\left[c_{45}\left(o_3-\Gamma_W^{(2)}\right)+c_{44}\left(o_3\Gamma_V^{(2)}-\sigma_3\Delta_V^{(2)}\right)-e_{14}\Gamma_\Phi^{(2)}\right]\sin(|\omega|\,\sigma_3 z)\right\}e^{|\omega|o_3 z}$$
$$\Omega_{01}^{(e)}(\omega,z)=\left\{\left[e_{15}\left(o_1-\Gamma_W^{(1)}\right)+e_{14}\left(o_1\Gamma_V^{(1)}-\sigma_1\Delta_V^{(1)}\right)+\in_{11}\Gamma_\Phi^{(1)}\right]\cos(|\omega|\,\sigma_1 z)\right.$$
$$\left.+\left[e_{15}\left(-\sigma_1+\Delta_W^{(1)}\right)-e_{14}\left(\sigma_1\Gamma_V^{(1)}+o_1\Delta_V^{(1)}\right)-\in_{11}\Delta_\Phi^{(1)}\right]\sin(|\omega|\,\sigma_1 z)\right\}e^{|\omega|o_1 z}$$
$$\Omega_{02}^{(e)}(\omega,z)=\left\{\left[e_{15}\left(\sigma_1-\Delta_W^{(1)}\right)+e_{14}\left(\sigma_1\Gamma_V^{(1)}+o_1\Delta_V^{(1)}\right)+\in_{11}\Delta_\Phi^{(1)}\right]\cos(|\omega|\,\sigma_1 z)\right.$$
$$\left.+\left[e_{15}\left(o_1-\Gamma_W^{(1)}\right)+e_{14}\left(o_1\Gamma_V^{(1)}-\sigma_1\Delta_V^{(1)}\right)+\in_{11}\Gamma_\Phi^{(1)}\right]\sin(|\omega|\,\sigma_1 z)\right\}e^{|\omega|o_1 z}$$
$$\Omega_{03}^{(e)}(\omega,z)=\left\{\left[e_{15}\left(o_3-\Gamma_W^{(2)}\right)+e_{14}\left(o_3\Gamma_V^{(2)}-\sigma_3\Delta_V^{(2)}\right)+\in_{11}\Gamma_\Phi^{(2)}\right]\cos(|\omega|\,\sigma_3 z)\right.$$
$$\left.+\left[e_{15}\left(-\sigma_3+\Delta_W^{(2)}\right)-e_{14}\left(\sigma_3\Gamma_V^{(2)}+o_3\Delta_V^{(2)}\right)-\in_{11}\Delta_\Phi^{(2)}\right]\sin(|\omega|\,\sigma_3 z)\right\}e^{|\omega|o_3 z}$$
$$\Omega_{04}^{(e)}(\omega,z)=\left\{\left[e_{15}\left(\sigma_3-\Delta_W^{(2)}\right)+e_{14}\left(\sigma_3\Gamma_V^{(2)}+o_3\Delta_V^{(2)}\right)+\in_{11}\Delta_\Phi^{(2)}\right]\cos(|\omega|\,\sigma_3 z)\right.$$
$$\left.+\left[e_{15}\left(o_3-\Gamma_W^{(2)}\right)+e_{14}\left(o_3\Gamma_V^{(2)}-\sigma_3\Delta_V^{(2)}\right)+\in_{11}\Gamma_\Phi^{(2)}\right]\sin(|\omega|\,\sigma_3 z)\right\}e^{|\omega|o_3 z}$$
$$\Omega_{11}^{(e)}(\omega,z)=-i\cdot\mathrm{sgn}(\omega)\left\{\left[e_{31}+e_{36}\Gamma_V^{(1)}+e_{33}\left(o_1\Gamma_W^{(1)}-\sigma_1\Delta_W^{(1)}\right)\right.\right.$$
$$\left.-\in_{33}\left(o_1\Gamma_\Phi^{(1)}-\sigma_1\Delta_\Phi^{(1)}\right)\right]\cos(|\omega|\,\sigma_1 z)-\left[e_{36}\Delta_V^{(1)}+e_{33}\left(o_1\Delta_W^{(1)}+\sigma_1\Gamma_W^{(1)}\right)\right.$$
$$\left.\left.-\in_{33}\left(o_1\Delta_\Phi^{(1)}+\sigma_1\Gamma_\Phi^{(1)}\right)\right]\sin(|\omega|\,\sigma_1 z)\right\}e^{|\omega|o_1 z}$$
$$\Omega_{12}^{(e)}(\omega,z)=-i\cdot\mathrm{sgn}(\omega)\left\{\left[\left[e_{36}\Delta_V^{(1)}+e_{33}\left(o_1\Delta_W^{(1)}+\sigma_1\Gamma_W^{(1)}\right)\right.\right.\right.$$
$$\left.-\in_{33}\left(o_1\Delta_\Phi^{(1)}+\sigma_1\Gamma_\Phi^{(1)}\right)\right]\cos(|\omega|\,\sigma_1 z)+\left[e_{31}+e_{36}\Gamma_V^{(1)}+e_{33}\left(o_1\Gamma_W^{(1)}-\sigma_1\Delta_W^{(1)}\right)\right.$$
$$\left.\left.\left.-\in_{33}\left(o_1\Gamma_\Phi^{(1)}-\sigma_1\Delta_\Phi^{(1)}\right)\right]\sin(|\omega|\,\sigma_1 z)\right\}e^{|\omega|o_1 z}$$
$$\Omega_{13}^{(e)}(\omega,z)=-i\cdot\mathrm{sgn}(\omega)\left\{\left[e_{31}+e_{36}\Gamma_V^{(2)}+e_{33}\left(o_3\Gamma_W^{(2)}-\sigma_3\Delta_W^{(2)}\right)\right.\right.$$
$$\left.-\in_{33}\left(o_3\Gamma_\Phi^{(2)}-\sigma_3\Delta_\Phi^{(2)}\right)\right]\cos(|\omega|\,\sigma_3 z)-\left[e_{36}\Delta_V^{(2)}+e_{33}\left(o_3\Delta_W^{(2)}+\sigma_3\Gamma_W^{(2)}\right)\right.$$
$$\left.\left.-\in_{33}\left(o_3\Delta_\Phi^{(2)}+\sigma_3\Gamma_\Phi^{(2)}\right)\right]\sin(|\omega|\,\sigma_3 z)\right\}e^{|\omega|o_3 z}$$
$$\Omega_{14}^{(e)}(\omega,z)=-i\cdot\mathrm{sgn}(\omega)\left\{\left[\left[e_{36}\Delta_V^{(2)}+e_{33}\left(o_3\Delta_W^{(2)}+\sigma_3\Gamma_W^{(2)}\right)\right.\right.\right.$$
$$\left.-\in_{33}\left(o_3\Delta_\Phi^{(2)}+\sigma_3\Gamma_\Phi^{(2)}\right)\right]\cos(|\omega|\,\sigma_3 z)+\left[e_{31}+e_{36}\Gamma_V^{(2)}+e_{33}\left(o_3\Gamma_W^{(2)}-\sigma_3\Delta_W^{(2)}\right)\right.$$
$$\left.\left.\left.-\in_{33}\left(o_3\Gamma_\Phi^{(2)}-\sigma_3\Delta_\Phi^{(2)}\right)\right]\sin(|\omega|\,\sigma_3 z)\right\}e^{|\omega|o_3 z}$$

4. *Expressions of* $\Theta_j(\omega,z)(j=1,2,3,4)$ *appearing in Eq. (40)*
For Case A

$$\Theta_j(\omega,z)=-i\cdot\mathrm{sgn}(\omega)g(o_j)e^{|\omega|o_j z},\ j=1,2,3,4$$

For Case B

$$\Theta_j(\omega, z) = -i \cdot \mathrm{sgn}(\omega) g(o_j) e^{|\omega| o_j z}, \quad j = 1, 2$$
$$\Theta_3(\omega, z) = -i \cdot \mathrm{sgn}(\omega) \left[\Gamma_W \cos(|\omega|\, \sigma_3 z) - \Delta_W \sin(|\omega|\, \sigma_3 z)\right] e^{|\omega| o_3 z}$$
$$\Theta_4(\omega, z) = -i \cdot \mathrm{sgn}(\omega) \left[\Delta_W \cos(|\omega|\, \sigma_3 z) + \Gamma_W \sin(|\omega|\, \sigma_3 z)\right] e^{|\omega| o_3 z}$$

For Case C

$$\Theta_1(\omega, z) = -i \cdot \mathrm{sgn}(\omega) \left[\Gamma_W^{(1)} \cos(|\omega|\, \sigma_1 z) - \Delta_W^{(1)} \sin(|\omega|\, \sigma_1 z)\right] e^{|\omega| o_1 z}$$
$$\Theta_2(\omega, z) = -i \cdot \mathrm{sgn}(\omega) \left[\Delta_W^{(1)} \cos(|\omega|\, \sigma_1 z) + \Gamma_W^{(1)} \sin(|\omega|\, \sigma_1 z)\right] e^{|\omega| o_1 z}$$
$$\Theta_3(\omega, z) = -i \cdot \mathrm{sgn}(\omega) \left[\Gamma_W^{(2)} \cos(|\omega|\, \sigma_3 z) - \Delta_W^{(2)} \sin(|\omega|\, \sigma_3 z)\right] e^{|\omega| o_3 z}$$
$$\Theta_4(\omega, z) = -i \cdot \mathrm{sgn}(\omega) \left[\Delta_W^{(2)} \cos(|\omega|\, \sigma_3 z) + \Gamma_W^{(2)} \sin(|\omega|\, \sigma_3 z)\right] e^{|\omega| o_3 z}$$

References

1. Chen, W.Q.: On piezoelectric contact problem for a smooth punch. Int. J. Solids Struct. **37**(16), 2331–2340 (2000)
2. Chung, M.Y., Ting, T.C.T.: Line force, charge and dislocation in angularly inhomogeneous anisotropic piezoelectric wedges and spaces. Philos. Mag. A. **71**, 1335–1343 (1995)
3. Ding, H.J., Chen, B., Liang, J.: General solutions for coupled equations for piezoelectric media. Int. J. Solids Struct. **33**(16), 2283–2298 (1996)
4. Ding, H.J., Wang, G.Q., Chen, W.Q.: Green's functions for a two-phase infinite piezoelectric plane. Proc. R. Soc. Lond. A. **453**, 2241–2257 (1997)
5. Ding, H.J., Wang, G.Q., Chen, W.Q.: A boundary integral formulation and 2D fundamental solutions for piezoelectric media. Comp. Mech. Appl. Mech. Eng. **158**(1–2), 65–80 (1998)
6. Erdogan, F.: Mixed boundary value problems in mechanics. In: Nemat-Nasser, S. (ed.) Mechanics Today, vol. 4, pp. 1–86. Pergamon Press, New York (1978)
7. Fan, H., Sze, K.Y., Yang, W.: Two-dimensional contact on a piezoelectric half-space. Int. J. Solids Struct. **33**, 1305–1315 (1996)
8. Giannakopoulos, A.E., Suresh, S.: Theory of Indentation of piezoelectric materials. Acta Mater. **47**(7), 2153–2164 (1999)
9. Guler, M.A., Erdogan, F.: Contact mechanics of graded coatings. Int. J. Solids Struct. **41**, 3865–3889 (2004)
10. Guler, M.A., Erdogan, F.: The frictional sliding contact problems of rigid semi-parabolic and cylindrical stamps on graded coatings. Int. J. Mech. Sci. **49**, 161–182 (2007)
11. Johnson, K.L.: Contact Mechanics. Cambridge University Press, Cambridge (1985)
12. Karapetian, E., Kachanov, M., Kalinin, S.V.: Nanoelectromechanics of piezoelectric indentation and applications to scanning probe microscopy of ferroelectric materials. Philos. Mag. **85**, 017–1051 (2005)
13. Ke, L.L., Wang, Y.S., Yang, J., Kitipornchai, S.: Sliding frictional contact analysis of functionally graded piezoelectric layered half-plane. Acta. Mech. **209**, 249–268 (2010)
14. Makagon, A., Kachanov, M., Kalinin, S.V., Karapetian, E.: Indentation and frictional sliding of spherical and conical punches into piezoelectric half-space. Phys. Rev. B. **76**(14), 064115 (2007)
15. Matysiak, S.: Axisymmetric problem of punch pressing into piezoelectro-elastic half space. Bull. Pol. Acad. Sci. Tech. **33**(1–2), 25–34 (1985)
16. Podilchuk, Y.N., Tkachenko, V.F.: The contact problem of electroelasticity for a flat punch with semi-parabolic cross-section. Int. Appl. Mech. **35**(11), 1096–1103 (1999)
17. Ramirez, G.: Frictionless contact in a layered piezoelectric media characterized by complex eigenvalues. Smart Mater. Struct. **15**, 1287–1295 (2006)
18. Ramirez, G., Heyliger, P.: Frictionless contact in a layered piezoelectric half-space. Smart Mater. Struct. **12**, 612–625 (2003)
19. Sosa, H.A., Castro, M.A.: On concentrated loads at the boundary of a piezoelectric half-plane. J. Mech. Phys. Solids **42**(7), 1105–1122 (1994)
20. Tiersten, H.F.: Linear Piezoelectric Plate Vibrations. Plenum, New York (1969)
21. Vel, S.S., Batra, R.C.: Three-dimensional analytical solution for hybrid multilayered piezoelectric plates. J. Appl. Mech. **67**(3), 558–567 (2000)
22. Wang, B.L., Han, J.C.: A circular indenter on a piezoelectric layer. Arch. Appl. Mech. **76**, 367–379 (2006)
23. Wang, B.L., Han, J.C., Du, S.Y., Zhang, H.Y., Sun, Y.G.: Electromechanical behavior of a finite piezoelectric layer under a flat punch. Int. J. Solids Struct. **45**(25–26), 6384–6398 (2008)
24. Zhou, Y.T., Lee, K.Y.: Thermo-electro-mechanical contact behavior of a finite piezoelectric layer under a sliding punch with frictional heat generation. J. Mech. Phys. Solids **59**, 1037–1061 (2011)